Co-expression clustering across flower development identifies modules for diverse floral forms in *Achimenes* (Gesneriaceae)

Wade R Roberts[1,2], Eric H Roalson[1]

[1] School of Biological Sciences, Washington State University, Pullman, WA, United States
[2] Current address: Biological Sciences, University of Arkansas, Fayetteville, AR, United States

Corresponding Author:
Wade Roberts[1]
Biological Sciences, University of Arkansas, SCEN 601, Fayetteville, AR, 72701, United States
Email address: wader@uark.edu

Abstract

Background. Genetic pathways involved with flower color and shape are thought to play an important role in the development of flowers associated with different pollination syndromes, such as those associated with bee, butterfly, or hummingbird pollination. Because pollination syndromes are complex traits that are orchestrated by multiple genes and pathways, the gene networks have not been explored. Gene co-expression networks provide a systems level approach to identify important contributors to floral diversification.

Methods. RNA-sequencing was used to assay gene expression across two stages of flower development (an early bud and an intermediate stage) in 10 species of *Achimenes* (Gesneriaceae). Two stage-specific co-expression networks were created from 9503 orthologs and analyzed to identify module hubs and the network periphery. Module association with bee, butterfly, and hummingbird pollination syndromes was tested using phylogenetic mixed models. The relationship between network connectivity and evolutionary rates (d_N/d_S) was tested using linear models.

Results. Networks contained 65 and 62 modules that were largely preserved between developmental stages and contained few stage-specific modules. Over a third of the modules in both networks were associated with flower color, shape, and pollination syndrome. Within these modules, several hub nodes were identified that related to the production of anthocyanin and carotenoid pigments and the development of flower shape. Evolutionary rates were decreased in highly connected genes and elevated in peripheral genes.

Discussion. This study aids in the understanding of the genetic architecture and network properties underlying the development of floral form and provides valuable candidate modules and genes for future studies.

Introduction

Flowers display a diverse range of colors, shapes, and sizes, and understanding the ecological and genetic factors contributing to their diversity across angiosperms has long been a major goal in biology. Often this diversity has been attributed to pollinator-mediated selection (Stebbins 1970; O'Meara et al. 2016; Gervasi and Schiestle 2017) and the relationship between a plant and its mode of pollination is considered to be one of the key innovations contributing to angiosperm diversification (Faegri and van der Pijl 1979; Fenster et al. 2004; van der Niet and Johnson 2012; Barrett 2013; Sauquet and Magallón 2018). Most plants evolved to rely on biotic or abiotic means in order to move pollen and ensure reproductive success (Faegri and van der Pijl 1979; Fenster et al. 2004). These biotic pollinators are often attracted to flowers that contain specific traits, such as red flowers that provide high nectar rewards for bird visitors (Cronk and Ojeda 2008) or the ultraviolet markings on some flowers that attract bee visitors (Papiorek et al 2016). A wide range of floral traits are thought to contribute to successful pollination, such as color (Sletvold et al. 2016), odor (Piechowski et al. 2010), nectar composition (Amorim et al. 2013), and time of flowering (Cortés-Flores et al. 2017). The genetic basis for these and other traits and their role in floral and pollination syndrome divergence has been examined extensively in model systems, particularly in *Mimulus* (Bradshaw et al. 1998; Yuan et al. 2016) and *Petunia* (Hoballah et al. 2007; Hermann et al. 2015), and more recently in many non-model systems (Wessinger et al. 2014; Alexandre et al. 2015).

Among the most widely used large-scale experimental approaches to investigate genome function are transcriptome analyses (Pickrell et al. 2010; Raherison et al. 2015), particularly in non-model organisms where no reference genome or functional genomics data exists. Changes in expression often result from the combinatorial action of genetic regulatory pathways orchestrating development and responses to environmental stimuli. Therefore, the transcriptome can be viewed as a link between the genotype and phenotype and may be acted upon through selection (Romero et al. 2012; Prasad et al. 2013). As changes in gene expression may underlie many of the phenotypic changes between species (Brawand et al. 2011; Romero et al. 2012; Uebbing et al. 2016), studying the transcriptome may shed light on important pathways and targets of selection. Phenotypic changes can frequently arise through functional changes in conserved developmental pathways among closely related species. For example, changes in enzyme function and transcriptional regulation of the anthocyanin pathway has been implicated frequently across angiosperms in the evolution of red flowers (Des Marais and Rausher 2010; Smith and Rausher 2011). It is now recognized that most genes act as members of biological pathways or of co-regulated modules (Hollender et al. 2014; Ma et al. 2018).

Here, we undertake a comparative study of gene expression during flower development in the genus *Achimenes*. This group is a member of the diverse African violet family (Gesneriaceae) and distributed throughout Mexico and Central America. *Achimenes* is a young lineage (*c*. 7-12 Mya; Roalson and Roberts 2016) known for its floral diversity (Figure 1), a

feature thought to be associated with speciation (Ramírez Roa 1987; Roalson et al. 2003). Four pollination syndromes are found in *Achimenes,* including melittophily (bees), psychophily (butterflies), euglossophily (female euglossine bees), and ornithophily (hummingbirds) (Figure 2). These syndromes have traditionally been defined on the basis of flower color and flower shape (Figure 2; Ramírez Roa 1987) and recently through pollinator observations (Martén-Rodríguez et al. 2015; Ramírez-Aguirre et al. 2019). Currently there have been pollinator observations made for four *Achimenes* species: *A. antirrhina* (hummingbirds, *Amazilia beryllina*), *A. flava* (bees, Anthophoridae), *A. obscura* (bees, *Trigona fulviventris*), and *A. patens* (unidentified butterflies) (Martén-Rodriguez et al. 2015; Ramírez-Aguirre et al. 2019). Based on these observations and the floral traits of these species (Figure 2), we can hypothesize the likely pollinators for the other *Achimenes* species (Figure 2; Table 1). Repeated origins and transitions between these pollination syndromes have been hypothesized in *Achimenes* (Roalson et al. 2003), making this small lineage an attractive system to understand the genetic and ecological factors underlying floral diversification.

In this study, we aimed to characterize and compare patterns of gene co-expression during flower development across 10 *Achimenes* species. So far, few studies have investigated the genetic basis of floral development in the Gesneriaceae family (Alexandre et al. 2015; Roberts and Roalson 2017). Given that bee, butterfly, and hummingbird pollination syndromes evolved in parallel across *Achimenes,* we hypothesized that: (1) distinct sets of co-expressed genes would correlate to each syndrome during flower development, and (2) genes in pathways involved with flower color and shape may be central in each network during flower development. Using a comparative transcriptome approach, we clustered a shared set of 9503 orthologs into two different co-expression networks, each corresponding to two stages of flower development: an early bud stage and an intermediate stage prior to anthesis. This strategy allowed us to compare gene co-expression patterns temporally. We compared these networks and tested whether gene co-expression clusters correlated with different floral traits (pollination syndrome, flower color, flower shape, corolla spurs). We also tested whether network properties, such as connectivity and expression, influence evolutionary constraints. Our results allowed us to quantify the extent of shared gene co-expression among closely related species and to identify pathways and genes that may be associated with the repeated evolution of flower types underlying pollinator specificity.

Materials & Methods

Plant materials

Ten of the 26 currently recognized species in *Achimenes* were sampled: five from Clade 1 and five from Clade 2 (Figure 2). These species were chosen based on their hypothesized close relationships and their diversity in floral form (Figure 1; Roalson et al. 2003). On the basis of previous molecular studies (Roalson and Roberts 2016), two species were chosen as outgroups to represent related lineages: *Eucodonia verticillata* and *Gesneria cuneifolia* (Figures 1-2). All

119 selected species were grown in standard greenhouse conditions at Washington State University,
120 under 16-hour days, 24-27°C, and 80-85% humidity.
121 Whole flower buds from two stages of flower development were sampled for each
122 species: an immature bud stage (Bud stage; Figure 1) and an intermediate stage before anthesis
123 (D stage; Figure 1). Our definitions of the floral developmental stages in *Achimenes* were
124 adapted from the stages determined for *Antirrhinum majus,* which uses a morphological and
125 temporal framework (Vincent and Enrico 2004). The Bud stage represents the smallest
126 reproductive bud distinguishable from vegetative buds, having lengths between 1-2 mm (Figure
127 1). The appearance is marked by the emergence of the floral primordia, no accumulation of
128 anthocyanin pigments, and no elongation or growth of corolla tissue cells. The D stage represents
129 a halfway point between the Bud and a pre-anthesis flower, where the length is about half the
130 length of a fully developed flower (Figure 1). Its appearance is marked by the accumulation of
131 anthocyanins in the corolla tissue, the cells have elongated in the corolla tube, and trichomes
132 have emerged. Corolla spurs are found only in *A. grandiflora* and *A. patens*, and the spur begins
133 development during the D stage as an outward growth of the corolla in the opposite direction
134 from the tube opening (Figure 1).
135 Each stage was sampled with two or three biological replicates, contributing four or six
136 samples for each species. The bud stage was chosen to represent a baseline level of gene
137 expression when floral phenotypes are largely similar between species that could then be
138 compared to the intermediate stage where floral phenotypes diverge and many important
139 pathways involved in flower development and pigmentation show increased expression levels
140 (Roberts and Roalson 2017). All tissues were immediately frozen into liquid nitrogen and stored
141 at -80°C.
142
143 **RNA extraction and RNA-seq library construction**
144 Total RNA was extracted from frozen tissue using the RNEasy Plant Kit (Qiagen) and
145 ribosomal depleted RNA samples were prepared using the RiboMinus Plant Kit (Thermo Fisher
146 Scientific). Stranded libraries were prepared using the NEBNext Ultra Directional RNA Library
147 Kit (New England Biolabs), barcoded, and pooled based on nanomolar concentrations. Library
148 quality and quantity were assessed using the Qubit (dsDNA HS assay; Thermo Fisher Scientific)
149 and BioAnalyzer 2100 (Agilent). The library pool was sequenced across 4 lanes of an Illumina
150 HiSeq2500 for paired-end 101 bp reads at the Genomics Core Lab at Washington State
151 University, Spokane. All new sequence data were deposited in the NCBI Sequence Read Archive
152 (BioProject: PRJNA435759).
153 Single replicate libraries for four of the species in the current study (*A. cettoana, A.*
154 *erecta, A. misera,* and *A. patens*) were previously sequenced for the same two timepoints (Bud
155 and D stages) (Roberts and Roalson 2017). These samples were combined with the newly
156 generated data to assembly de novo transcriptomes and perform co-expression clustering. This
157 data was deposited in the NCBI Sequence Read Archive (BioProject: PRJNA340450).
158

Transcriptome assembly

Per base quality, adapter contamination, and per base sequence content of raw reads was assessed with FastQC tools (http://bioinformatics.babraham.ac.uk/projects/fastqc). One library (AT6) returned poor yields and low-quality reads and was excluded from further analyses. Trimmomatic v.0.36 (Bolger et al. 2014) was then used to remove contaminating adapter sequences and dynamically trim low-quality bases (ILLUMINACLIP:TruSeq3-PE-2.fa:2:30:10 HEADCROP:13 LEADING:3 TRAILING:3 SLIDINGWINDOW:4:15 MINLEN:50). Trimmed reads derived from an individual species were combined and de novo assembled into contigs using Trinity (--SS_lib_type RF; Grabherr et al. 2011; Haas et al. 2013), generating a reference transcriptome for each species. Sequence redundancy was reduced with CDHIT-EST (-c 0.99 -n 5; Li and Godzik 2006). Open reading frames were then predicted for each transcriptome assembly with TransDecoder (Haas et al. 2013) using a BLASTp search against the SwissProt database (www.uniprot.org) to maximize sensitivity. Finally, transcriptome assembly completeness was assessed using BUSCO (Simão et al. 2015) against a set of single-copy plant orthologs (embryophyte_odb10 dataset).

Orthogroup inference

To help facilitate orthogroup inference, transcriptome assemblies from flowers in *Sinningia eumorpha* and *S. magnifica* were downloaded and combined with our assemblies (https://doi.org/10.5061/dryad.4r5p1; Serrano-Serrano et al. 2017a). *Sinningia* is closely related to our focal lineage in the Neotropical Gesneriaceae (Roalson and Roberts 2016). To identify orthogroup sequences across all 14 species, we used a modified version of the approach described in Yang and Smith (2014). All peptide sequences were clustered using an all-by-all BLASTp search performed using DIAMOND (--evalue 1e-6; Buchfink et al. 2014) and results were clustered using MCL v14-137 (-I 1.4; Enright et al. 2002). Homolog clusters were aligned using MAFFT v7.271 (--genafpair --maxiterate 1000; Katoh and Standley 2013) and alignments were trimmed using Phyutility v2.7.1 (-clean 0.1; Smith and Dunn 2008). Codon alignments were then produced for each cluster using PAL2NAL v14 (Suyama et al. 2006) and maximum-likelihood trees were constructed using FastTree v2.1.8 (Price et al. 2010) using the GTR model. Trees were then trimmed to exclude branches >10 times longer than its sister or longer than 0.2 substitutions per site. Final homolog group alignments were created from the trimmed trees using MAFFT and used for final homolog tree inference using RAxML v8.2.9 (Stamatakis 2014) and the GTRGAMMA model. Orthogroups were inferred from the final homolog trees using the rooted ingroup (RT) method of Yang and Smith (2014), using *S. eumorpha* and *S. magnifica* as outgroups. Homolog trees were trimmed to include at least 2 ingroup species, resulting in 83595 orthogroups.

Quantifying gene expression

Trimmed reads for each sample were aligned to the corresponding transcriptome assembly to quantify expression using default parameters in Kallisto v0.43.0 (Bray et al. 2016).

The resulting counts for each contig were matched with the inferred orthogroups derived above, creating two separate matrices for the Bud and D stage samples. In the resulting gene expression matrices, rows corresponded to orthogroups and columns corresponded to individual samples (Supplemental Data). Counts for the Bud and D stage samples were separately transformed using variance-stabilizing transformation implemented in the Bioconductor package DESeq2 (Love et al. 2014) and quantile normalized using the Bioconductor package preprocessCore (Bolstad 2018). Lastly, counts for both stages were separately corrected for confounding effects, such as batch or species effects, using principal component regression with the 'sva_network' function in the Bioconductor package sva (Parsana et al. 2019).

Co-expression networks and identification of modules

The Bud and D stage RNAseq data was clustered into gene co-expression networks using the R package WGCNA (Langfelder and Horvath 2008). Prior to network construction, orthogroups were filtered to remove any with >50% missing values or <0.3 expression variance. In total, 9503 orthogroups common to both Bud and D stage data were used to construct separate networks for each stage. Parameters for the Bud stage network were as follows: power = 18, networkType = "signed", corType = "bicor", maxPOutliers = 0.05, TOMType = "signed", deepSplit = 2, mergeCutHeight = 0.25. For the D stage network, the following parameters were used: power = 16, networkType = "signed", corType = "bicor", maxPOutliers = 0.05, TOMType = "signed", deepSplit = 2, mergeCutHeight = 0.25. Soft-thresholding powers for each network ("power" parameter) were chosen as the lowest value such that the scale free topology model fit (R^2) was ≥ 0.9 (Supplemental Data). Signed networks consider positively correlated nodes connected, while unsigned networks consider both positively and negatively correlated nodes connected (van Dam et al. 2018). We used signed networks here ("networkType" and "TOMType" parameters) because this type is considered more robust to biological functions with more specific expression patterns (Mason et al. 2009; Song et al. 2012). Unsigned networks can capture only strong correlations and many negative regulatory relationships in biological systems are weak or moderate (Ritchie et al. 2009). Biweight midcorrelation ("corType" parameter) was used as this method is often more robust than Pearson correlation and more powerful than Spearman correlation (Song et al. 2012). All other WGCNA parameters were kept at their default values.

Module eigengenes and orthogroup connectivity were calculated in each network separately using the 'moduleEigengenes' and 'intramodularConnectivity' functions in WGCNA, respectively. The module eigengene is defined as the first principal component of a module and represents the gene expression profile of a sample within a module (Langfelder and Horvath 2008). Connectivity refers to the sum of connection strengths a node has to other network nodes.

Module hub genes (defined as the most highly connected nodes within a module) were identified in both networks based on module membership (kME) scores > 0.9, calculated using the 'signedKME' function of WGCNA. kME is defined as the correlation between the expression levels of a gene and the module eigengene (Horvath and Dong 2008). Additionally,

using connectivity measures, we defined peripheral genes in each network as the lowest 10% of connected nodes.

We tested whether Bud stage modules were preserved in the D stage and vice versa using module preservation statistics in WGCNA (Langfelder et al. 2011). Median Rank and Zsummary statistics were computed using the 'modulePreservation' function of WGCNA, using 200 permutations (Langfelder et al. 2011). Median rank statistics were compared to the "gold" module, which consists of 1000 randomly selected orthogroups. Modules with a lower median rank exhibit stronger preservation than modules with a higher median rank. Zsummary scores > 10 indicate strong evidence of preservation and scores < 2 indicate no evidence of preservation.

Phylogeny

We previously inferred a phylogeny for the 12 sampled species using 1306 single-copy orthologs identified from the same transcriptome dataset used here (Roberts and Roalson 2018). For comparative analyses of module-trait relationships, we randomly sampled 50 single-copy ortholog gene trees and rescaled branch lengths to be proportional to time (ultrametric) using the 'chronos' function in the R package ape (Paradis et al. 2004). Bootstrap support was 100 for nearly every branch in the Roberts and Roalson (2018) phylogeny, therefore we chose to use randomly sampled ortholog trees to account for phylogenetic uncertainty.

Module and trait relationship

We correlated external traits (e.g., red flower color) with the module eigengenes using a phylogenetic Markov Chain Monte Carlo method, implemented in the R packages MCMCglmm (Hadfield 2010) and mulTree (Guillerme and Healy 2014). These analyses were performed individually for each module in both the Bud and D stage networks. Three floral traits and pollination syndrome were coded: primary flower color (purple, red, white, yellow), flower shape (funnelform, salverform, tubular), corolla spur (absent, present), and syndrome (bee, butterfly, hummingbird). We fit a multivariate mixed model with a non-informative prior, where the shape and scale parameters equal 0.001, and residual variance was fixed. Analyses were performed over the 50 randomly selected ortholog trees to account for phylogenetic uncertainty. A phylogenetic model was used to account for any interspecific non-dependency in the dataset by using a random effects structure that incorporated a phylogenetic tree model. Floral traits were set as categorical response variables and the module eigengenes were set as the predictor variable. For each tree, two MCMC chains were run for 250k generations and discarding the first 50k as burn-in. This process was run individually over each module in both the Bud and D stages. We checked for convergence between model chains using the Gelman-Rubin statistic (Gelman and Rubin 1992). Potential scale reduction values were all less than 1.1 and effective sample sizes for all fixed effects were greater than 400. We considered fixed effects to be statistically significant when the probabilities in the 95% credible region did not include zero (Supplemental Figures 3-6).

Evolutionary rate analysis

Codon alignments of the filtered orthogroups (n=9503) were produced using PAL2NAL v14 (Suyama et al. 2006). Subsequent alignments and corresponding gene trees were used as input to the codeml package in PAML v4.9 (Yang 2007) to estimate d_N/d_S (omega, ω). d_N/d_S for each orthogroup was estimated using a one-ratio model (model = 0, NSsites = 0), providing a single estimate for each orthogroup to match other single orthogroup metrics, such as connectivity. If d_N/d_S values were exceptionally large (= 999) because of zero synonymous differences, those values were removed from the dataset.

First, we performed linear regression (LM) to test the effect of orthogroup connectivity, average expression levels, and their interactions (explanatory variables) on the estimated d_N/d_S values (main effect), LM = d_N/d_S ~ connectivity * expression. This was performed using the lm function in R with 10000 bootstrap pseudoreplicates. Second, we ran two-sample t-tests with 10000 permutations to test whether hub nodes and periphery nodes in each network had lower (for hubs) or higher (for periphery) d_N/d_S values than all background nodes. Third, we fit a LM with 10000 bootstrap pseudoreplicates to test whether modules associated with a pollination syndrome (bee, butterfly, or hummingbird; see Results below) had increased d_N/d_S values, LM = d_N/d_S ~ syndrome. For all LM and permutation analyses, d_N/d_S, connectivity, and expression values were log transformed to reach a normal distribution before being processed. Analyses were performed separately for each network using the separately estimated connectivity and expression levels.

Functional annotation and GO enrichment analysis

Filtered orthogroups (n=9503) were annotated based on a search against all green plant proteins in the SwissProt database (release 2018_07; The UniProt Consortium 2017) using Diamond BLASTp (--evalue 1e-6). Results were used to assign annotations and gene ontology (GO) terms. GO enrichment analyses were performed using the R package TopGO with the default "weight01" algorithm with the recommended cutoff of $p < 0.05$ (Alexa et al. 2006). Enriched GO term redundancy was removed and summarized using the semantic similarity measures implemented in the REVIGO web server (Supek et al. 2011).

Data and code availability

Raw sequencing reads are available from the NCBI Sequence Read Archive under BioProjects: PRJNA435759 and PRJNA340450. Data and code for all analyses can found from https://drive.google.com/open?id=1pvzw1t1pObY_kAEYmxQ484PCTuEWrsrb.

Results

Transcriptome assembly

Twelve transcriptomes were sequenced (72 libraries) and assembled in 12 species after sampling across two floral developmental stages (Supplemental Table 1). The transcriptomes had

319 an average assembly length of 244.9 Mb (± 33.9 Mb), an average of 217,510 (± 47k) transcripts,
320 and an average N50 length of 1988 bp (± 306 bp). Between 22,942 and 33,501 putative genes
321 were detected with 2.34 (± 0.35) putative isoforms. BUSCO identified an average of 87% of the
322 complete, conserved single-copy plant orthologs (Supplemental Table 1). Our focus in our
323 comparative study was on the presence of conserved orthologs, and not on the presence of
324 taxonomically restricted genes, which are not likely preserved across species.
325
326 **Constructing the co-expression network for 12 species**
327 We identified 83595 orthologous clusters (orthogroups), each containing at least 2
328 species. After removing 74092 orthogroups with too many missing values (> 50% missing) or
329 low expression variance (< 0.3 variance) and keeping common orthogroups shared between the
330 Bud and D stages, 9503 orthogroups were used to construct two co-expression networks using
331 the weighted gene correlation network analysis (WGCNA) approach. Modules of co-expressed
332 orthogroups are inferred using the expression profiles of each sample regardless of species.
333 Clustering identified 65 and 62 co-expression modules in the Bud and D stage networks,
334 respectively (Figure 3; Supplemental Table 2). Module size in the Bud stage ranged from 22
335 (module ME63) to 592 (ME1) orthogroups (mean = 146) and ranged from 21 (ME61) to 704
336 (ME1) orthogroups (mean = 153) in the D stage. Out of the 9503 orthogroups, 7845 (83%) and
337 8735 (92%) were assigned to modules in each network.
338 The remaining unassigned genes from each network that were not placed into a well-
339 defined module were assigned to the ME0 module by WGCNA. Despite being unplaced, these
340 orthogroups may still be functionally relevant within each network. Unassigned genes in the
341 ME0 module were enriched for many processes, including transcription (Bud, n = 173; D, n =
342 84) and organ development (D, n = 55), among other functions (Supplemental Tables 3-4).
343 We tested whether modules in the Bud stage were preserved in the D stage, and vice
344 versa. Overall, preservation of modules between the Bud and D stage networks was high. Eight
345 of the 65 Bud stage modules (ME46, ME62, ME44, ME57, ME42, ME41, ME55, ME40) were
346 not strongly preserved in the D stage, while only 1 of the 62 D stage modules (ME59) was not
347 strongly preserved in the Bud stage (Supplemental Table 5). These patterns suggest that these
348 non-preserved modules may play unique roles within their network. Among the 8 Bud stage-
349 specific modules were many orthogroups related to primary cell growth, meristem identity and
350 differentiation, stamen development, and flowering (Supplemental Table 3). In the single D
351 stage-specific module were many orthogroups related to methylation, flowering, and carotenoid
352 biosynthesis (Supplemental Table 4). Despite the relatively high preservation, correspondence
353 between module membership in the Bud and D stages was moderate (Figure 4). Orthogroup
354 module membership tended to shift between each network. For example, most members of
355 module ME15 in the Bud stage are transferred to modules ME3 and ME7 in the D stage (Figure
356 4).
357 We defined network hubs (the most highly connected nodes within a module) with
358 module membership (kME) scores > 0.9. Using this definition, all modules in each network

359 contained at least one hub, with the percentage of hubs ranging from 1% to 24% of orthogroups
360 in a module (Figures 5-6; Supplemental Table 6). Of the 632 and 691 hubs identified in the Bud
361 and D stages, a significant portion (110) were shared between networks (Fisher's Exact Test,
362 odds ratio = 3.02, $P < 0.001$). Functional enrichment of hubs in the Bud stage revealed that many
363 were involved in the regulation of development and metabolic processes (n = 40), transport and
364 protein localization (n = 39), biosynthetic processes (n = 19), and DNA methylation (n = 7),
365 consistent with the notion that hubs usually play important roles in integrating other genes during
366 network evolution (Ravasz et al. 2002) (Table 2). In the D stage, hubs were enriched for
367 functions related to translation (n = 33), transport (n = 9), ethylene and abscisic acid signaling
368 pathways (n = 17), carotenoid and anthocyanin biosynthetic processes (n = 11), and the
369 regulation of gene expression (n = 20), among others (Table 2).
370 Nodes in the periphery of each network were loosely defined by considering them to be
371 the lowest 10% connected ($connectivity_{Bud} < 2.824$, $connectivity_{D} < 4.651$). These definitions
372 identified 951 periphery nodes (Supplemental Table 7), of which 301 were peripheral in both
373 networks (Fisher's Exact Test, odds ratio = 5.67, $P < 0.001$). These periphery nodes in the Bud
374 stage were enriched for functions related to reproductive structure development (n = 75),
375 transport and localization (n = 107), and signaling (n = 389), among others (Table 3). In the D
376 stage, the periphery was enriched for functions related to the regulation of flower development (n
377 = 64), the regulation of flowering time (n = 18), the regulation of flavonoid biosynthesis (n = 7),
378 and cell fate specification (n = 12), among others (Table 3). Greater than expected numbers of
379 peripheral nodes in the D stage were related to regulation (Fisher's exact test, odds ratio = 1.191,
380 $p = 0.02752$) and transcription (Fisher's exact test, odds ratio = 1.370, $p = 0.001549$). In contrast,
381 there were no differences in the expected number of peripheral nodes related to regulation
382 (Fisher's exact test, odds ratio = 0.955, $p = 0.7044$) or transcription (Fisher's exact test, odds
383 ratio = 1.047, $p = 0.3549$) in the Bud stage.
384
385 **Modules associated with floral traits**
386 We calculated module eigengenes, single values which represent the gene expression
387 profiles of a sample within a module (Supplemental Figures 1-2). The extent of module
388 involvement in various biological processes can be tested by correlating eigengenes with external
389 traits, such as flower color. We tested the relationship between the module eigengenes and the
390 four floral traits (pollination syndrome [bee, butterfly, hummingbird], flower color [purple, red,
391 yellow, white], flower shape [funnelform, salverform, tubular], and corolla spurs [absence,
392 presence]), while controlling for any phylogenetic bias in the dataset using a phylogenetic mixed
393 model (Figures 5-6; Supplemental Figures 3-6). We also examined whether eigengene values (>
394 0.1 or < -0.1) in single species contributed to a strong correlation or whether eigengene values (>
395 0.1 or < -0.1) in multiple species contributed to a strong correlation (Figures 5-6; Supplemental
396 Figures 3-6). We considered there to be strong evidence for trait association when a significant
397 correlation from MCMCglmm was coupled with elevated eigengene (> 0.1) or decreased
398 eigengene (< -1.0) expression in multiple species that shared any of the significant traits.

399 Likewise, weak evidence for trait association was considered when the MCMCglmm results
400 were significant, but only a single species or no species sharing the significant traits had elevated
401 (> 0.1) or decreased (< -1.0) eigengene expression. WGCNA does not use trait information when
402 inferring modules, so modules that correlated strongly with any floral trait were inferred without
403 a priori knowledge.
404 *Pollination syndrome*—We included 3 species with the bee pollination syndrome (*A.*
405 *candida, A. misera,* and *E. verticillata*), 4 species with the butterfly pollination syndrome (*A.*
406 *cettoana, A. grandiflora, A. longiflora,* and *A. patens* 'Major'), and 5 species with the
407 hummingbird pollination syndrome (*A. admirabilis, A. antirrhina, A. erecta, A. pedunculata,* and
408 *G. cuneifolia*) (Figure 2; Table 1). These pollination syndromes are traditionally defined in
409 *Achimenes* and other gesneriads based on primary flower color, flower shape, and the presence
410 of corolla spurs (Wiehler 1983; Ramírez Roa 1987; Roalson et al. 2003). Expression of 23 (35%)
411 and 21 (34%) modules were positively associated with the pollination syndromes in the Bud and
412 D stage networks, consisting of 2967 and 2880 orthogroups, respectively. (Figures 5-6). There
413 were 3 (4.6%), 7 (10.8%), and 13 (20%) modules associated with bee, butterfly, and
414 hummingbird pollination syndrome in the Bud stage network, while 1 (1.5%), 8 (12.9%), and 12
415 (19.4%) modules were associated with the same syndromes in the D stage. Modules were never
416 associated with more than one syndrome. Butterfly and hummingbird syndromes were never
417 correlated to the same modules and were often correlated in opposite directions (i.e., butterfly
418 was positive correlated and hummingbird was negative correlated).
419 Among the 3 modules that were correlated to the bee pollination syndrome in the Bud
420 stage were many orthogroups involved in hormone signaling pathways (particularly ethylene and
421 abscisic acid, n = 14), cell wall and lipid biosynthesis (n = 7), photomorphogenesis (n = 2),
422 nitrogen compound metabolism (n = 4), and the transport of potassium and monocarboxylic
423 acids (n = 5) (Table 4). In contrast, the 1 module correlated to the bee pollination syndrome in
424 the D stage was enriched for different functions from the Bud stage, including the positive
425 regulation of molecular functions and response to biotic stimuli (n = 7), phospholipid catalysis (n
426 = 2), xyloglucan biosynthesis (n = 2), mRNA stability and catalysis (n = 5), and chromatin
427 modification (n = 4) (Table 5).
428 The 7 modules correlated to the butterfly pollination syndrome in the Bud stage
429 contained orthogroups involved in RNA splicing (n = 16), fertilization (n = 3), DNA methylation
430 (n = 2), cell growth and shoot formation (n = 8), the development of organ boundaries (n = 3),
431 and stress responses (n = 83) (Table 4). Within the 8 modules correlated with butterfly
432 pollination in the D stage were orthogroups enriched for functions in photorespiration (n = 7),
433 microtubule organization (n = 5), chromatin silencing (n = 3), red and far-red light responses (n
434 = 3), modified amino acid biosynthesis and metabolism (n = 10), and mRNA transport (n = 9)
435 (Table 5).
436 Thirteen modules were correlated to the hummingbird pollination syndrome in the Bud
437 stage and the orthogroups were enriched for numerous functions, including many developmental
438 processes (Table 4). These modules were enriched for floral whorl development (n = 12), RNA

439 and mRNA modifications (n = 19), cell growth and division (n = 54), organelle assembly (n = 3),
440 transportation of carbohydrates and potassium (n = 22), and responses to external stimuli (n =
441 17) (Table 4). Many of the same enrichments were seen in the 12 modules correlated to the
442 hummingbird pollination syndrome in the D stage. These modules had enrichments for floral
443 whorl development (n = 14), cell polarity and proliferation (n = 8), adaxial/abaxial specification
444 (n = 8), organ formation (n = 3), the regulation of growth (n = 26), and endosperm development
445 (n = 6). Additionally, these modules had enrichment for RNA and mRNA modification (n = 79),
446 transcription (n = 3), protein-DNA complex formation (n = 7), signaling (n = 25), and UV
447 response (n = 9) (Table 5).
448 *Flower color*—Primary flower color is closely associated to pollination syndrome in
449 *Achimenes* (Ramírez Roa 1987; Roalson et al. 2003), and we identified 26 (40%) and 17 (27%)
450 modules associated to any flower color in the Bud and D stage networks, consisting of 2935 and
451 1500 orthogroups respectively (Figures 5-6). Red and yellow are associated with hummingbird
452 pollination, purple with butterfly pollination, and white with bee pollination. In the Bud stage,
453 there were 14 (21.5%), 11 (16.9%), and 1 (1.5%) module associated with red, purple, or yellow
454 flower color. In the D stage, no modules were associated with yellow, but 8 (12.9%) and 9
455 (14.5%) modules were associated with red or purple flower color. In both networks, no modules
456 were corelated to white flower color. Similar to syndrome, purple and red flower color were
457 never associated with the same modules and were always correlated in opposite directions.
458 The 14 modules associated with red flowers in the Bud stage overlapped significantly
459 with the modules associated with the hummingbird pollination syndrome in the Bud stage and
460 contained the same functional enrichments (Table 4; Supplemental Table 8). However, in the 8 D
461 stage modules associated with red flowers, the orthogroups were enriched for functions involved
462 in flower morphogenesis (n = 8), cell wall modification (n = 3), positive regulation of gene
463 expression (n = 14), and histone modification (n = 7), among others (Supplemental Table 8).
464 Within the 11 modules associated with purple flowers in the Bud stage were orthogroups
465 enriched for transcription (n = 14), meristem initiation (n = 4), DNA methylation (n = 3),
466 fertilization (n = 5), ethylene signaling (n = 5), response to biotic stimuli (n = 55), and others
467 (Supplemental Table 8). In contrast, the 9 modules associated with purple flowers in the D stage
468 were enriched for orthogroups involved in anther and endosperm development (n = 9),
469 translation (n = 4), the regulation of developmental processes (n = 9), lipid modification (n = 8),
470 cell division (n = 3), and hormone signaling (gibberellic acid and jasmonic acid, n = 6), among
471 many other processes (Supplemental Table 8).
472 A single module (ME36) was associated with yellow flower color, only in the Bud stage,
473 and contained few orthogroups involved in floral meristem determinacy (n = 1), floral organ
474 identity (n = 1), gene silencing (n = 1), sulfur compound biosynthesis (n = 2), and vegetative
475 phase change (n = 1) (Supplemental Table 8).
476 *Flower shape*—Flower shape is also important but not as closely associated to pollination
477 syndromes as primary flower color in *Achimenes* (Ramírez Roa 1987; Roalson et al. 2003).
478 Flowers with bee pollination tend to have funnelform flowers, butterfly pollinated flowers all

479 have salverform flowers, and hummingbird pollinated flowers have either salverform or tubular
480 flowers (Table 2). Overall, there were 14 (22%) and 13 (21%) modules associated with any of
481 the flower shapes in the Bud and D stages, consisting of 2940 and 2504 orthogroups,
482 respectively (Figures 5-6). Here, there were 1 (1.5%), 8 (12.3%), and 5 (7.7%) modules whose
483 expression correlated to funnelform, salverform, or tubular flowers in the Bud stage (Figure 5).
484 Fewer modules were correlated in the D stage network, but expression in 1 (1.6%), 7 (12.3%),
485 and 5 (8.1%) modules were associated with funnelform, salverform, and tubular shapes (Figure
486 4). No modules were positively associated with more than one flower shape.
487 Only two modules were associated with funnelform flowers, one in the Bud stage and the
488 other in the D stage, and these were enriched for functions related to ethylene signaling (n = 3),
489 lipid biosynthesis (n = 3), chromatin modification (n = 4), cell wall organization (n = 2), and
490 many metabolic processes (Supplemental Table 8). Within the 8 modules associated with
491 salverform flowers in the Bud stage, there were many orthogroups involved in mRNA processing
492 and modification (n = 50), ovule development (n = 7), chlorophyll biosynthesis (n = 4), and the
493 regulation of flower development (n = 20) (Supplemental Table 8). In the D stage, the 7 modules
494 associated with salverform flowers contained orthogroups involved in chromatin silencing (n =
495 7), anthocyanin biosynthesis (n = 10), cell cycle and cell division (n = 95), stamen development
496 (n = 12), auxin biosynthesis (n = 7), and transport (n = 17) (Supplemental Table 8).
497 Among the 5 modules associated with tubular flowers in the Bud stage were orthogroups
498 enriched for functions in the positive regulation of transcription and organelle assembly (n = 13),
499 RNA processing (n = 5), xylem development (n = 4), metabolism (n = 12), and many
500 biosynthetic processes (Supplemental Table 8). In the 5 modules associated with tubular flowers
501 in the D stage were enrichments for floral whorl development (n = 6), positive regulation of gene
502 expression (n = 15), mRNA modification (n = 5), and signaling (n = 12) (Supplemental Table 8).
503 *Corolla spurs*—The presence of corolla spurs is found only on butterfly pollinated
504 species, two of which were included: *A. grandiflora* and *A. patens* (Figure 1; Table 1). There was
505 expression in 5 (7.7%) modules associated with spurs in the Bud stage network, while only 1
506 (1.6%) module was associated in the D stage network (Figures 3-4). Within the 5 modules
507 associated with corolla spurs in the Bud stage were orthogroups related to miRNA processing (n
508 = 4), mRNA splicing (n = 9), the regulation of signal transduction pathways (n = 16), and pollen
509 tube growth (n = 6) (Supplemental Table 8). In the single module associated with corolla spurs in
510 the D stage (ME53) were very few orthogroups involved in microtubule organization (n = 2),
511 stamen development (n = 1), the positive regulation of cell division (n = 1), flavonoid
512 biosynthesis (n = 1), and indole acetic acid metabolism (n = 1) (Supplemental Table 8).
513 *Non-associated*—There were 13 and 9 modules not associated with any traits in the Bud
514 and D stage networks, respectively (Figures 5-6). Three of these modules in the Bud stage were
515 not-preserved in the D stage (modules ME46, ME44, and ME41; Figures 5-6; Supplemental
516 Table 5). The 9 non-associated modules in the D stage were also not associated with any traits in
517 the Bud stage (Figures 5-6) and the orthogroups had overlapping enrichments for many essential
518 processes (Supplemental Table 8). These modules were enriched for orthogroups involved in the

519 development of the inflorescence, stamens, and floral organs, biosynthesis of vitamins and
520 nucleotides, photosynthesis and photosynthetic electron transport, metabolism of phosphate
521 compounds, and cell surface receptor signaling (Supplemental Table 8). Numerous orthogroups
522 were also involved in the positive regulation of reproduction, the negative regulation of growth,
523 and the regulation of heterochronic development, histone methylation, and gibberellic acid
524 mediated signaling (Supplemental Table 8).
525
526 **Evolutionary rates correlate to network location**
527 We ran several analyses to explore how several network variables may affect
528 evolutionary rates of the orthogroups within each network (as measured by d_N/d_S). First, we tested
529 the effects of orthogroup connectivity, expression levels, and their interaction on the d_N/d_S values
530 (Supplemental Table 7). Results indicated a collective effect between connectivity and
531 expression on d_N/d_S in both the Bud stage (LM, $F(3,9548) = 92.58$, p = 0, $\eta^2 = 0.03$) and the D
532 stage networks (LM, $F(3,9548) = 78.36$, p = 0, $\eta^2 = 0.02$). We found that orthogroup connectivity
533 was negatively correlated with d_N/d_S in the Bud stage network (LM, t = -16.31, p = 0) and the D
534 stage network (LM, t = -15.13, p = 0) (Figure 7), while expression was positively correlated with
535 d_N/d_S in the Bud stage (LM, t = 2.12, p = 0.0344) and not in the D stage (LM, t = 1.51, p =
536 0.1324) (Supplemental Figure 7). The interaction between connectivity and expression also
537 indicated a marginal dependency of both predictors on d_N/d_S in the Bud stage (LM, t = -2.022, p =
538 0.0433) but not in the D stage network (LM, t = -1.823, p = 0.0683). These patterns have been
539 observed in model species and may be universal to all eukaryotes.
540 Second, we tested whether the nodes we defined as hubs in each network had lower d_N/d_S
541 values, suggestive of increased evolutionary constraint (Supplemental Table 9). Hubs are
542 considered to functionally significant and may control large portions of the network. We found
543 that the hubs in the Bud stage network had lower d_N/d_S than all background genes (Two-sample t-
544 test, $t(679.31) = 7.0934$, p = 1.65e-12, Cohen's d = 0.383; Permutation t-test. mean diff. = 0.266,
545 p = 0.0001) (Supplemental Figure 8). Similarly, hubs in the D stage network also had lower d_N/d_S
546 than all background genes (Two-sample t-test, $t(755.91) = 4.1918$, p = 1.55e-05, Cohen's d =
547 0.206; Permutation t-test, mean diff. = 0.143, p = 0.0001) (Supplemental Figure 8).
548 Third, we tested whether the most peripheral nodes (the lowest 10% connected nodes)
549 had higher d_N/d_S values, which may suggest relaxed evolutionary constraint (Supplemental Table
550 9). These nodes are loosely connected within the network and their roles may be more apt to
551 fluctuate during evolution and development. These peripheral genes had higher d_N/d_S than all
552 background genes in the Bud stage network (Two-sample t-test, $t(1487.70) = -10.272$, p = 0,
553 Cohen's d = -0.253; Permutation t-test, mean diff. = -0.176, p = 0.0001) and the D stage network
554 (Two-sample, $t(1512.30) = -10.387$, p = 0, Cohen's d = -0.252; Permutation t-test, mean diff. = -
555 0.175, p = 0.0001) (Supplemental Figure 8).
556 Lastly, we tested whether modules correlated with bee, butterfly, or hummingbird
557 pollination syndromes showed increased evolutionary rates over the non-associated modules.
558 Results indicated a very weak effect of syndrome association on d_N/d_S in the Bud network (LM,

559 $F(3,9548) = 5.186$, p = 0.001406, $\eta^2 = 0.0016$) and the D network (LM, $F(3,9548) = 4.277$, p =
560 0.005038, $\eta^2 = 0.0013$) (Supplemental Table 9). Only bee syndrome associated modules had
561 marginally lower d_N/d_S values in both networks (Bud stage, LM, t = -3.58, p = 0.000346; D stage,
562 LM, t = -2.508, p = 0.0122). Butterfly associated modules had marginally lower d_N/d_S only in the
563 D stage (LM, t = -2.548, p = 0.0108), while hummingbird associated modules did not have any
564 effect in either network.
565

566 ## Discussion

567 Here we report on patterns of gene co-expression across two stages of flower
568 development in 12 species of *Achimenes, Eucodonia,* and *Gesneria*. Our comparative and
569 phylogenetic context allowed us to reveal gene co-expression patterns across a group of closely
570 related plant species that correlated to diverse pollination syndromes and floral traits, including
571 flower color, flower shape, and corolla spurs. Our results suggest floral forms that are associated
572 with bee, butterfly, and hummingbird pollinator groups are correlated with many co-expression
573 modules. We found that nearly a third of modules in each network (23 and 21 modules in the
574 Bud and D stages, respectively) had evidence for association with the three pollination
575 syndromes (Figures 5-6). In our analysis, large fractions of our 9503 orthogroups set could be
576 partitioned into modules (Figure 3), network hubs and peripheral nodes identified (Supplemental
577 Tables 6-7), and several orthogroups were identified for their potential importance in floral
578 phenotypic differentiation. Lastly, orthogroup position in each network (measured by
579 connectivity) had an association with evolutionary rate (d_N/d_S) (Figure 7). These analyses provide
580 a first overview of floral transcriptional architecture across members of the same genus that
581 display diverse floral forms.
582

583 **Hub nodes contain important candidates for floral form**

584 To date, a large number of studies conducted in diverse angiosperm systems, have found
585 that many genes are associated with flower development (Quattrocchio et al. 1999; Howarth et
586 al. 2011). Despite evidence for extensive gene/genome duplications that could expand the
587 genetic repertoire (Tang et al. 2008), many recent studies have suggested that the generation of
588 novel genes is rare (Patterson et al. 2009; De Smet et al. 2013). Thus, the evolution and
589 development of diverse floral forms may predominantly occur through the co-option of existing
590 pathways (Preston et al. 2011). To our knowledge, gene co-expression network analyses have not
591 been previously used across multiple species in a non-model lineage to understand flower
592 development and evolution.
593 Hub nodes (genes) are considered to be conserved, highly connected nodes that are
594 central to network architecture and may directly orchestrate numerous biological processes
595 (Ravasz et al. 2002; Hu et al. 2016; Mähler et al. 2017). Our analyses identified over 600 gene
596 nodes as hubs within each network, the majority of which were only hubs within a specific floral
597 stage. These hub nodes tended to have lower d_N/d_S estimates, suggesting that they not prone to
598 rapid evolutionary change (Supplemental Table 9). Unsurprisingly, hub nodes in the Bud stage

599 were enriched for many processes related to early flower development, including cell growth,
600 leaf formation, and photosystem assembly (Table 2). Similarly, hub nodes in the D stage were
601 enriched for genes that may be related the development of distinct floral forms, including
602 carotenoid biosynthesis, anthocyanin biosynthesis, and cell morphogenesis (Table 2). Within this
603 context of flower development, we identified a number of hubs that we consider important
604 candidates for involvement in the production of flower color and the development of floral form.
605 Many of these candidates were considered previously (Roberts and Roalson 2017) as potentially
606 important for the diversification of floral form in *Achimenes*. Undoubtedly, this list of hubs
607 contains many genes that may important for other biological traits that we do not consider here,
608 such as scent, nectar, and pollen production.
609 *Anthocyanin biosynthesis*—Anthocyanins are common floral pigments that produce red,
610 purple, and blue colors and are produced via the highly conserved flavonoid biosynthetic
611 pathway (Holton and Cornish 1995). With a few exceptions, all anthocyanins are produced from
612 three precursor molecules: pelargonidin, cyanidin, and delphinidin (Grotewold 2006). There are
613 six enzymatic reactions required for the production of anthocyanins and many also serve as
614 branching points for the production of flavonoids, lignins, flavonols, and other phenolics that
615 have roles in stress response and physiology (Winkel-Shirley 2002; Tahara 2007). We identified
616 four homologs of anthocyanin biosynthetic pathway enzymes as network hubs: flavonoid 3'-
617 hydroxylase (*F3'H*; cluster8703_1rr.inclade1.ortho3; module ME12), dihydroflavonol 4-
618 reductase (*DFR*; cluster5082_1rr.inclade1.ortho6; module ME48), flavonoid 3',5'-
619 methyltransferase (*FAOMT*; cluster11783_1rr.inclade1.ortho1.tre; module ME32), and flavonol
620 3-O-glucosyltransferase (*UFOG*; cluster8241_2rr.inclade1.ortho2.tre; module ME1).
621 These 4 enzymes are involved in distinct steps during anthocyanin production and
622 chemical modification in floral tissue. Activity of *F3'H* directs the pathway toward the
623 production of cyanidins and quercetin (Grotewold 2006). Cyanidin can accumulate in floral
624 tissue as a purple-hued pigment, while quercetin plays a large role in various stress-related
625 physiological functions (Pollastri and Tattini 2011), including response to high light and UVB
626 radiation (Gerhardt et al. 2008) and antioxidant properties (Rice-Evans et al. 1996). Therefore,
627 *F3'H* as an important hub in the networks makes sense given its enormous pleiotropic role in
628 various physiological responses. Just prior to the production of anthocyanins, *DFR* catalyzes the
629 reaction to produce pelargonidins, cyanidins, and delphinidins from the precursor molecules
630 dihydrokaempferol, dihydroquercetin, and dihyrdomyricetin, respectively (Grotewold 2006).
631 Shifts in *DFR* expression, function, and substrate specificity have been implicated in many
632 evolutionary transitions in flower color (Smith et al. 2013; Wu et al. 2013).
633 Further modifications to anthocyanins, such as methylation, glycosylation, and acylation,
634 produce a wide variety of compounds and hues (Wessinger and Rausher 2012). We identified
635 homologs to both a methyltransferase (*FAOMT*) and glucosyltransferase (*UFOG*) as hubs in the
636 networks. Methylation of anthocyanins have been widely studied in petunia (Provenzano et al.
637 2014), grapes (Hugueney et al. 2009) and tree peony (Du et al. 2015), demonstrating that
638 methylation can impact the hue, either shifting it more toward purple (Sakata et al. 1995) or

639 sometimes red (Tanaka et al. 2008). Glycosylation stabilizes anthocyanins molecules for
640 subsequent transfer to acidic vacuoles (Saito and Yamazaki 2002), increasing their solubility,
641 and influencing their color variability by inter- and intra-molecular stacking (Springob et al.
642 2003). Finding homologs of *FAOMT* and *UFOG* as network hubs reflect the importance of
643 anthocyanin modification for different flower color hues among *Achimenes* species.
644 *Carotenoid biosynthesis*—Carotenoids are red, orange, and yellow pigments that are
645 produced in plastids and are essential for photosynthesis, but also accumulate as secondary
646 metabolites in flowers to attract pollinators (Kevan and Baker 1983). Floral and fruit carotenoids
647 can also be used to produce volatile apocarotenoids, which may further enhance plant-animal
648 interactions during pollination and seed dispersal (Dudareva et al. 2006). They may also serve as
649 precursors to the production of the hormone abscisic acid and strigalactones that are involved in
650 many plant developmental processes (Rosas-Saavedra et al. 2016). We identified 4 homologs of
651 carotenoid biosynthetic pathway enzymes as network hubs: geranylgeranyl pyrophosphate
652 synthase (*GGPPS*; cluster10945_2rr.inclade1.ortho1.tre; module ME35), phytoene
653 dehydrogenase (*PDS*; cluster13048_1rr.inclade1.ortho1.tre; module ME4), lycopene beta cyclase
654 (*LCYB*; cluster13774_1rr.inclade1.ortho1.tre; module ME7), and capsanthin-capsorubin synthase
655 (*CCS*; cluster13583_1rr.inclade1.ortho2.tre; module ME6).
656 Each of these 4 enzymes catalyzes reactions during different steps of carotenoid
657 production. *GGPPS* produces the main precursor molecular geranylgeranyl pyrophosphate
658 (GGPP) to carotenoid biosynthesis that is produced as the end-product of the plastid
659 methylerythritol 4-phosphate (MEP) pathway. Two GGPP molecules are then condensed into
660 phytoene and undergoes four successive dehydrogenations and isomerizations to produce
661 lycopene. *PDS* catalyzes the first two desaturation steps that transform the colorless phytoene
662 into the red-colored lycopene. *PDS* is a rate-limiting enzyme in carotenoid biosynthesis
663 (Chamovitz et al. 1993) and down-regulation has been shown to lead to large accumulations of
664 phytoene (Busch et al. 2002) and decreases in total carotenoid, chlorophyll, and photosynthetic
665 efficiency (Wang et al. 2009).
666 Lycopene is the main starting compound for a large variety of carotenoids. *LCYB* takes
667 lycopene as a substrate and subsequently produces beta-carotene. Many plants use tissue-specific
668 isoforms of *LCYB* genes that are expressed in fruits or flowers that often correlate with the
669 accumulation of beta-carotene or downstream xanthophylls (Ronen et al. 2000; Ahrazem et al.
670 2010; Devitt et al. 2010). Beta-carotenes are hypothesized to be the primary carotenoids in
671 *Achimenes* flowers (Roberts and Roalson 2017). Another functionally related carotenoid cyclase
672 enzyme is *CCS* (or neoxanthin synthase, *NSY*) which catalyzes the final step in the carotenoid
673 pathway and converts the yellow-colored violaxanthin into neoxanthin (Parry and Horgan 1991).
674 Both violaxanthin and neoxanthin can be further used for producing the plant hormone abscisic
675 acid (Neuman et al. 2014). Both enzymes are likely functionally important in the developing
676 flowers for the biosynthesis of beta-carotene and xanthophylls.
677 *Flower development*—Very few studies have so far investigated the molecular
678 mechanisms involved in the development of flower shape in the Gesneriaceae (Gao et al. 2008;

679 Zhou et al. 2008; Alexandre et al. 2015). However, extensive work has been done in model
680 organisms, such as *Arabidopsis thaliana* and *Antirrhinum majus,* which can provide insight into
681 the potential roles that many transcription factors might play in determining floral organ identity
682 and shape in *Achimenes*. Among the network hubs, we identified several homologs that are likely
683 involved in floral organ development, including mixta (*MIXTA*;
684 cluster8699_1rr.include1.ortho3.tre; modules ME5 and ME8), agamous (*AG*;
685 cluster7311_1rr.include1.ortho3.tre; module ME23), globosa (*GLO*;
686 cluster2750_1rr.include1.ortho3.tre; module ME37), and tcp4 (*TCP4*;
687 cluster12380_1rr.include1.ortho2.tre; module ME22).
688 Petal identity and petal surface morphology are both thought to be important components
689 for pollinator attraction (Noda et al. 1994; Whitney et al. 2011). *MIXTA* was first characterized
690 from *Antirrhinum* and controls the development of the conical cell shape in the petal epidermis
691 (Noda et al. 1994). Consequently, *MIXTA* and *MIXTA*-like genes have been characterized in
692 other model systems, such as *Arabidopsis* and *Mimulus* for their similar role in epidermal cell
693 morphogenesis (Baumann et al. 2007) as well as trichome development (Gilding and Marks
694 2010; Scoville et al. 2011). The homolog of *MIXTA* in our study was a hub node in both
695 networks, suggesting it might play an important role throughout flower development in
696 determining petal surface morphology.
697 Early floral organ determination requires the involvement of several MADS-box
698 transcription factors, such as *AG* and *GLO*. We identified homologs of *AG* as a hub in the Bud
699 stage and *GLO* as a hub in the D stage (Supplemental Table 7). *AG* has been shown in
700 *Arabidopsis* to be expressed in early flower development in order to terminate meristem activity
701 and promote the development of stamens and carpels, while working in combination with
702 *APETALA3, PISTILLATA,* and *SEPALLATA* (Gómez-Mena et al. 2005). More recently homologs
703 of *AG* were demonstrated to be involved in nectary development in both *Arabidopsis* and
704 *Petunia* (Morel et al. 2018), another floral trait important for plant-pollinator interaction. *GLO*
705 was first characterized in *Antirrhinum* and *Arabidopsis* and is also involved with stamen identity,
706 as well as petal identity (Tröbner et al. 1992; Goto and Meyerowitz 1994). Outside of these
707 model systems, its expression patterns and role in the evolution of complex floral forms have
708 been examined in numerous plant lineages, from monocots (Bartlett and Specht 2010) to
709 Solanaceae (Zhang et al. 2014). *AG* and *GLO* will be interesting candidates to begin exploring
710 further how petals, stamens, carpels, and nectary development in *Achimenes*.
711 Lastly, the homolog of *TCP4* was identified as a hub during the Bud stage, and may be
712 important for its potential role in petal development and cell proliferation. Looking into the
713 genetic factors regulating the elaboration of petal growth will be important for understanding
714 how corolla spurs develop in *Achimenes* (Figure 1). The role of *TCP4* been characterized in
715 *Arabidopsis* for its role in both petal growth, showing restricted expression to the developing
716 petal tissue (Nag et al. 2009). More recent work using gene regulatory networks in *Arabidopsis*
717 has shown that petal size is controlled by a *SEPALLATA3*-regulated miR319/*TCP4* module
718 (Chen et al. 2018). Outside of *Arabidopsis, TCP4* was also implicated for a having a role in the

719 development of the petal spur in *Aquilegia* (Yant et al. 2015). Therefore, considering both the
720 role for *TCP4* in petal and spur development demonstrated in *Arabidopsis* and *Aquilegia* and its
721 identification as a hub gene in our networks, we think this gene requires further interrogation.
722
723 **Peripheral genes are enriched for transcriptional regulators in later stages of development**
724 Peripheral nodes have low connectivity within co-expression networks (Supplemental
725 Table 7), tend to have higher rates of molecular evolution (Masalia et al. 2017), and have been
726 hypothesized to contribute more to evolutionary innovations than network hubs (Ichihashi et al.
727 2014). Of the 951 nodes we defined as peripheral in both Bud and D stage networks, roughly a
728 third were consistently peripheral under our definitions (lowest 10% connected; Supplemental
729 Table 7). After identifying the nodes with homologies to transcriptional regulators, we found
730 there was no difference in the expected number in the early Bud stage, while there were greater
731 than expected numbers of transcriptional regulators in the periphery of the D stage (see Results).
732 No such patterns existed when we tested these transcriptional regulators as hub genes. While
733 Mähler et al. (2017) found an enrichment for transcription factors among hub genes in a single
734 species network of *Populus tremula,* our results in a multi-species network find the opposite
735 pattern. Shifting the expression patterns of various genes and pathways can lead to phenotypic
736 divergence among closely related species (West-Eberhard 1989). This can be seen during later
737 stages of flower development when distinct traits, such as red or purple flower color, can appear
738 in different species due to shifting expression patterns within the anthocyanin biosynthetic
739 pathway (Smith and Rausher 2011). The connection between the apparent overabundance of
740 transcriptional regulators in later stages of flower development and the rapid phenotypic
741 divergence in floral form will need to be explored further.
742 Several notable peripheral nodes were identified for their potential involvement in
743 important floral processes (Supplemental Table 7). Three homologs were identified in the
744 periphery of the Bud stage with potential involvement in the determination of zygmorphic
745 (bilateral) floral symmetry: two homologs of divaricata (*DIV*;
746 cluster13684_1rr.include1.ortho1.tre, cluster8585_1rr.include1.ortho1.tre; ME26 and ME0) and
747 one homolog of dichotoma *(DICH*; cluster13245_1rr.include1.ortho1.tre; ME0). Bilateral
748 symmetry has been proposed as a mechanism that facilitates pollen transfer by insects (Galliot et
749 al. 2006). Both *DIV* and *DICH* are TCP transcription factors that were first characterized in
750 *Antirrhinum* (Almeida et al. 1997; Luo et al. 1996), and show localized expression to the ventral
751 and dorsal portions of the petal, respectively. *Achimenes* flowers at the Bud stage are lacking or
752 only just beginning to establish floral asymmetry and the relegation of both *DIV* and *DICH* to the
753 network periphery may reflect this small role. The role of these genes has not been studied in the
754 Gesneriaceae, but have been examined more recently in other non-model systems for their role in
755 the evolution of pollination syndromes (Zhang et al. 2010; Preston et al. 2011). Additionally, a
756 homolog of the homeobox wuschel gene (*WUS*; cluster9273_1rr.include1.ortho1.tre; module
757 ME0) was identified from the periphery of the D stage network. *WUS* was first characterized in
758 *Arabidopsis* for its role in meristem cell maintenance (Laux et al. 1996) and its expression is

759 localized only to the meristem (Mayer et al. 1998). Once the floral meristem has been initiated,
760 *WUS* starts to be repressed by *AG* (hub gene, described above) (Sun et al. 2009). The relegation
761 of *WUS* to the periphery in our networks at the D stage might then be expected given that it plays
762 such a prominent role during early floral development and the vegetative to reproductive
763 transition.
764
765 **Evolutionary rates are correlated to network connectivity**
766 Increased protein evolutionary rates during rapid diversification has been suggested in
767 other radiations of animals and plants (Kapralov et al. 2013; Brawand et al. 2014; Pease et al.
768 2016). Our study is among the first to examine patterns of network evolution across multiple
769 closely-related species of plants with multiple transitions in flower type and pollination
770 syndrome. Hummingbirds are hypothesized to have had an important influence on diversification
771 in Neotropical Gesneriaceae (Roalson and Roberts 2016; Serrano-Serrano et al. 2017b), while
772 the role of butterflies has not been explored. Modules correlated with hummingbird or butterfly
773 pollination syndromes did not exhibit clear increases or decreases in evolutionary rates compared
774 to other modules (Supplemental Table 9). Detecting selection is subject to many factors, such as
775 a gene's transcriptional abundance and its importance within the protein interaction network
776 (Lemos et al. 2005). For instance, we found that higher network connectivity was strongly
777 associated with lower evolutionary rates across both networks in our study (Figure 7;
778 Supplemental Table 9). This corroborates the recent results found in other eukaryotic systems
779 (Morandin et al. 2016; Masalia et al. 2017; Josephs et al. 2017; Mähler et al. 2017) while also
780 showing the apparent strength of correlation between connectivity and evolutionary rate differs
781 between studies and systems.
782 Network effects (such as the type of network analysis employed) and the expression
783 levels of highly abundant genes are known to affect evolutionary rates, potentially confounding
784 analysis of selection pressure (Krylov et al. 2003). We found that d_N/d_S in early development may
785 be dependent on both connectivity and expression levels, while this interactive effect was gone
786 during later development (Supplemental Table 9). As there are few highly connected genes
787 (hubs, which are important determinants of the observed network structure), a random mutation
788 would be less likely to affect such a gene. Changing the amino acid sequence of a hub gene
789 could have multiple associated effects, some deleterious (Hahn and Kern 2004; Luisi et al.
790 2015). In comparison, a random mutation would be more likely to affect a gene with lower
791 connectivity, while also resulting in variants with fewer negative consequences. The hub genes
792 have more direct interactions and are more likely to be essential and involved in more biological
793 processes, placing them under greater constraint.
794
795 **Numerous network modules correlated to floral form**
796 One primary use for gene co-expression network analyses is to identify modules of co-
797 expressed genes whose overall expression (as measured by the eigengene) may correlate with
798 different traits. These traits can be both qualitative or quantitative, such as social caste (Morandin

et al. 2016), seed oil production (Hu et al. 2016), or anther development (Hollender et al. 2014). While we tested only qualitative traits here, future studies could also correlate eigengene expression to quantitative variables such as nectary size or sucrose concentration, since these appear to be another important component of pollination syndrome delimitation (Perret et al. 2001; Katzer et al. 2019; Vandelook et al. 2019). Since our dataset was composed of samples from 12 species, we performed correlation analyses using a phylogenetic model to test whether module expression correlated to different flower colors, flower shapes, corolla spurs, and pollination syndromes. Nearly half of our modules in both networks had evidence for an association with these floral traits (Figures 5-6). There were no modules whose correlation to a pollination syndrome had increased eigengene expression in all species sharing that trait (Figures 5-6). Instead many modules with correlation to a trait showed a phylogenetic pattern with a shared increased eigengene expression among the most closely related species. For example, module ME23 in the Bud stage network had a correlation to butterfly pollination and increased eigengene expression in *A. cettoana* and *A. longiflora,* both members of Clade 1 (Figure 2). Our aim was to identify sets of co-expressed genes that would provide candidates for involvement in the development of these traits.

For instance, many of the candidate hubs we identified (see above) were found in modules that were correlated to one or multiple traits to which they might contribute, such as *PHAN* (module ME4, correlated to corolla spurs) and *DFR* (module ME48, correlated to hummingbird pollination and purple flowers) (Supplemental Table 2). Additionally, modules correlated to various floral traits were enriched for multiple genes that might be involved in the development of those traits (Supplemental Table 8). Module ME53 was correlated to the corolla spurs found in *A. grandiflora* and *A. patens* in the D stage network and was enriched for many genes involved in cell division and cell growth (Figure 6; Supplemental Table 4). Other times, modules were correlated to a specific trait but the enriched GO terms did not provide a clear idea of how these co-expressed orthogroups may contribute (Supplemental Tables 3-4). In our analyses, we considered relatively few traits and only focused on those that have traditionally been considered the most important for the differentiation of floral form in *Achimenes*, namely flower color, flower shape, and corolla spurs. Undoubtedly there are a myriad number of molecular and biochemical pathways that we have not considered here that underlie the development of these complex floral phenotypes. With the idea that networks represent complex systems of gene and protein interactions, it may be that these seemingly simple and generalized floral phenotypes are produced through much more complex means than many have previously considered.

Strengths and limitations of network analyses in non-model organisms

Our analysis covers genes with orthologs found in most species, representing a set of evolutionarily conserved genes. While no reference genome currently exists for Neotropical Gesneriaceae, we constructed, annotated, and presented de novo transcriptomes for 10 *Achimenes* species as well as 2 outgroup species, *E. verticillata* and *G. cuneifolia*. Our approach

839 enables functional genomic studies in this non-model system, but the potential for misassemblies
840 may bias our downstream results (Hornett and Wheat 2012). Using a gene tree-based approach to
841 carefully identify orthogroups, we focused our attention on conserved gene regulatory machinery
842 and not on taxonomically restricted genes. The latter may be involved in species-specific
843 functions. Nevertheless, it is worth noting that many recent studies have indicated that transitions
844 in floral form may be due to the shifting expression of genes found in conserved genetic
845 pathways (Wessinger and Rausher 2014). Taxonomically restricted genes are likely interacting
846 with existing regulatory pathways, and the manner in which they integrate into the co-expression
847 modules identified here will be a fascinating topic for future research. With extended sampling
848 within *Achimenes* we could infer species-specific co-expression networks and perform more
849 detailed cross-species comparisons. We expect that these taxonomically restricted genes may be
850 poorly connected with the network, which may allow for increased diversification.
851 We characterized gene expression patterns by sequencing RNA across two timepoints
852 during flower development. Previous gene expression experiments across three timepoints (early
853 Bud, intermediate D, and late Pre-anthesis stages) in four *Achimenes* species suggested that the
854 majority of differential gene expression occurred between the early Bud stage and the
855 intermediate D stage (Roberts and Roalson 2017). We believe our approach allows us to capture
856 dynamic transcriptional patterns during flower development for comparison across multiple
857 species. We found that the co-expression networks for the Bud and D stages were largely
858 preserved, despite there being a few stage specific modules (Supplemental Table 5). However,
859 this approach may greatly over-simplify the nature of transcriptional regulation in these species.
860 Organ- and structure-specific expression studies may have greater power to detect floral form-
861 specific differences, both in terms of the number of differentially expressed genes, and co-
862 expression network structure (Hollender et al. 2014; Suzuki et al. 2017; Shahan et al. 2018). As a
863 result, our data likely represents an underestimate of the true number of modules. Future studies
864 could focus on the comparative analysis of expression patterns in specific organs, such as the
865 petals, stigma, and stamens, and additional timepoints, which would provide greater functional
866 insight into the evolution, development, and diversification of these organs.
867 Network analysis represents a more complex approach than differential expression
868 analyses because it can capture system-level properties (Langfelder and Horvath 2008). Most
869 phenotypes involve interactions of proteins from diverse biochemical pathways. Although
870 inferred modules do not necessarily correspond to entire biochemical pathways, or other
871 components of cellular organization, the approach performs well in reconstructing the
872 complexity of protein-protein interaction networks (Allen et al. 2012). In many systems this
873 approach has succeeded in identifying candidate genes for various biological traits, for example
874 floral organ development in strawberry (Hollender et al. 2014; Shahan et al. 2018) or carotenoid
875 accumulation in carrots (Iorizzo et al. 2016). Our results demonstrate the difficulty in identifying
876 gene clusters that underlie highly correlated floral traits, especially in non-model systems, as
877 seen by the overlapping correlation of modules associated with flower shape and color (Figures
878 5-6). It has been shown in many plant systems that floral traits tend to be selected together by

879 pollinators (Cuartas-Domínguez and Medel 2010; Sletvold et al. 2010), making it challenging to
880 separate correlated modules from causal modules. Co-expression networks are foundationally
881 about correlations between genes (van Dam et al. 2018), making them useful in identifying novel
882 sets of genes that may be functionally relevant for trait of interest. Other approaches, such as
883 quantitative trait locus (QTL) analyses may provide more promise in identifying distinct genes
884 that are involved in the divergence of floral traits. QTL studies have already shown promise in
885 identifying genetic loci that underlie pollination syndrome divergence in *Mimulus* (Yuan et al.
886 2013), *Penstemon* (Wessinger et al. 2014), and *Rhytidophyllum* (Alexandre et al. 2015).
887 We were able to identify numerous candidate orthogroups involved in the development of
888 floral form in our non-model system. While no functional genomic data exists yet for *Achimenes,*
889 our annotations are based on the manually curated SwissProt database. De novo assemblies
890 provide important data for non-model organisms, but there can be biases introduced during
891 assembly and annotation due to potentially missing genes (Hornett and Wheat 2012). We
892 attempted to limit this bias by focusing only on shared orthogroups found in the majority (at least
893 6) of our sampled *Achimenes*. Applying this network-based approach to the diversification of
894 flowers across multiple species in *Achimenes*, we recovered distinct modules of co-expressed
895 genes that may underlie a range of floral phenotypic traits tied to different pollination
896 syndromes. Although our data come from whole flowers during development, and do not allow
897 us to test specific hypotheses regarding whether particular genes have shifted expression location
898 in the developing flower, they do suggest that there are conserved regulatory modules that may
899 have been co-opted in convergent flower types multiple times. It will be interesting to apply
900 network analyses to study floral diversification in additional lineages and examine how
901 conserved or divergent the patterns are across angiosperms.
902

903 ## Conclusions

904 Floral forms corresponding to bee, butterfly, and hummingbird pollination have evolved
905 multiple times across the Neotropical plant genus *Achimenes*. Genome-wide gene expression
906 estimates were taken from flowers in 12 species across two development stages in order to
907 construct, analyze, and compare stage-specific gene co-expression networks. We hypothesized
908 that numerous modules in each network would correlate to these pollination syndromes and that
909 central genes in the network may be candidates for involvement in the development of important
910 floral traits, such as flower color and shape. We found that nearly a third of modules were
911 correlated to the pollination syndromes and many more were correlated to different flower colors
912 and shapes. The outgroup species, *E. verticillata* (bee pollinated) and *G. cuneifolia*
913 (hummingbird pollinated), displayed correlation patterns similar to the ingroup species that
914 shared floral traits, suggesting that some co-expression patterns might be shared across
915 evolutionary distances. Several of the hub genes in the networks were homologs of the
916 anthocyanin and carotenoid biosynthetic pathways, important for the production of floral
917 pigments that attract different pollinators. A negative relationship between network connectivity
918 and d_N/d_S corroborates the findings in model systems that more centrally located nodes (likely

hubs) are under increased evolutionary constraint. We found that the less connected genes (peripheral) are under more relaxed constraints and contained numerous transcriptional regulators. Our results demonstrate the utility of applying co-expression network analyses in non-model plant lineages to begin identifying important modules and pathways that will be useful starting points for additional analyses into the evolution and development of floral form.

Acknowledgements

We thank Joanna Kelley, Amit Dhingra, and Andrew McCubbin for helpful comments that improved this work. Sequencing was performed at the Genomics Core Lab at Washington State University, Spokane, and the Genomics Sequencing and Analysis Facility at the University of Texas, Austin.

References

Ahrazem O, Rubio-Moraga A, López RC, Gómez-Gómez L. 2010. The expression of a chromoplast-specific lycopene beta cyclase gene is involved in high production of saffron's apocarotenoid precursors. J Exp Bot 61:105-119.

Alexa A, Rahnenführer J, Lengauer T. 2006. Improved scoring of functional groups from gene expression data by decorrelating GO graph structure. Bioinformatics 22:1600-1607.

Alexandre H, Vrignaud J, Mangin B, Joly S. 2015. Genetic architecture of pollination syndrome transition between hummingbird-specialist and generalist species in the genus Rhytidophyllum (Gesneriaceae). PeerJ 3:e1028.

Allen JD, Xie Y, Chen M, Girard L, Xiao G. 2012. Computing statistical methods for constructing large scale gene networks. PLOS One 7:e29348.

Almeida J, Rocheta M, Galego L. 1997. Genetic control of flower shape in Antirrhinum majus. Development 124:1387-1392.

Amorim FW, Galetto L, Sazima M. 2013. Beyond the pollination syndrome: nectar ecology and the role of diurnal and nocturnal pollinators in the reproductive success of Inga sessilis. Plant Biol 15:317-327.

Baumann K, Perez-Rodriguez M, Bradley D, Venail J, Bailey P, Jin H, Koes R, Roberts K, Martin C. 2007. Control of cell and petal morphogenesis by R2R3 MYB transcription factors. Development 134:1691-1701.

Barrett SC. 2013. The evolution of plant reproductive systems: how often are transitions irreversible? P Roy Soc B-Biol Sci 280: 20130913.

Bartlett ME, Specht CD. 2010. Evidence for the involvement of GLOBOSA-like gene duplications and expression divergence in the evolution of floral morphology in the Zingiberales. New Phytol 187:521-541.

Bolger AM, Lohse M, Usadel B. 2014. Trimmomatic: a flexible trimmer for Illumina sequence data. Bioinformatics 30:2114-2120.

Bolstad B. 2018. preprocessCore: A collection of pre-processing functions. R package version 1.46.0, https://github.com/bmbolstad/preprocessCore.

959 Bradshaw HD, Otto KG, Frewen BE, McKay JK, Schemske DW. 1998. Quantitative trait loci
960 affecting differences in floral morphology between two species of monkeyflower
961 (Mimulus). Genetics 149:367-382.
962 Brawand D, Soumillon M, Necsulea A, Julien P, Csárdi G, Harrigan P, Weier M, Liechti A,
963 Aximu-Petri A, Kircher M, Albert FW. 2011. The evolution of gene expression levels in
964 mammalian organs. Nature 478:343.
965 Brawand D, Wagner CE, Li YI, Malinsky M, Keller I, Fan S, Simakov O, Ng AY, Lim ZW,
966 Bezault E, Turner-Maier J. 2014. The genomic substrate for adaptive radiation in African
967 cichlid fish. Nature 513:375.
968 Bray NL, Pimentel H, Melsted P, Pachter L. 2016. Near-optimal probabilistic RNA-seq
969 quantification. Nat Biotechnol 34:525.
970 Buchfink B, Xie C, Huson DH. 2014. Fast and sensitive protein alignment using DIAMOND.
971 Nat Methods 12:59-60.
972 Busch M, Seuter A, Hain R. 2002. Functional analysis of the early steps of carotenoid
973 biosynthesis in tobacco. Plant Physiol 128:439-453.
974 Chamovitz D, Sandmann G, Hirschberg J. 1993. Molecular and biochemical characterization of
975 herbicide-resistant mutants of cyanobacteria reveals that phytoene desaturation is a rate-
976 limiting step in carotenoid biosynthesis. J Biol Chem 268:17348-17353.
977 Chen D, Yan W, Fu LY, Kaufmann K. 2018. Architecture of gene regulatory networks
978 controlling flower development in Arabidopsis thaliana. Nat Commun 9:1-13.
979 Cortés-Flores J, Hernández-Esquivel KB, González-Rodríguez A, Ibarra-Manríquez G. 2017.
980 Flowering phenology, growth forms, and pollination syndromes in tropical and dry forest
981 species: influence of phylogeny and abiotic factors. Am J Bot 104:39-49.
982 Cronk Q, Ojeda I. 2008. Bird-pollinated flowers in an evolutionary and molecular context. J Exp
983 Bot 59:715-727.
984 Cuartas-Domínguez M, Mendel R. 2010. Pollinator-mediated selection and experimental
985 manipulation of the flower phenotype in Chloraea bletioides. Funct Ecol 24:1219-1227.
986 Des Marais DL, Rausher MD. 2010. Parallel evolution at multiple levels in the origin of
987 hummingbird pollination flowers in Ipomoea. Evolution 64:2044-2054.
988 De Smet R, Adams KL, Vandepoele K, Van Montagu MC, Maere S, Van de Peer Y. 2013.
989 Convergent gene loss following gene and genome duplications creates single-copy
990 families in flowering plants. P Natl Acad Sci USA 110:2898-2903.
991 Devitt LC, Fanning K, Dietzgen RG, Holton TA. 2010. Isolation and functional characterization
992 of a lycopene β-cyclase gene that controls fruit colour of papaya (Carica papaya L.). J
993 Exp Bot 61:33-39.
994 Du H, Wu J, Ji KX, Zeng QY, Bhuiya MW, Su S, Shu QY, Ren HX, Liu ZA, Wang LS. 2015.
995 Methylation mediated by an anthocyanin O-methyltransferase is involved in purple
996 flower coloration in Paeonia. J Exp Bot 66:6563-6577.
997 Dudareva N, Negre F, Nagegowda DA, Orlova I. 2006. Plant volatiles: recent advances and
998 future perspectives. Cr Rev Plant Sci 25:417-440.

999 Enright AJ, Van Dongen S, Ouzounis CA. 2002. An efficient algorithm for large-scale detection
1000 of protein families. Nucleic Acids Res 30:1575-1584.
1001 Faegri K, van der Pijl L. 1979. *Principles of Pollination Ecology*. Oxford: Pergamon Press.
1002 Fenster CB, Armbruster WS, Wilson P, Dudash MR, Thomson JD. 2004. Pollination syndromes
1003 and floral specialization. Annu Rev Ecol Evol S 35:375-403.
1004 Galliot C, Stuurman J, Kuhlemeier C. 2006. The genetic dissection of floral pollination
1005 syndromes. Curr Opin Plant Biol 9:78-82.
1006 Gao Q, Tao JH, Yan D, Wang YZ, Li ZY. 2008. Expression differentiation of CYC-like floral
1007 symmetry genes correlated with their protein sequence divergence in Chirita heterotricha
1008 (Gesneriaceae). Dev Genes Evol 218:341-351.
1009 Gelman A, Rubin DB. 1992. Inference from iterative simulation using multiple sequences. Stat
1010 Sci 7:457-472.
1011 Gerhardt KK, Lampi MA, Greenberg BM. 2008. The effect of far-red light on plant growth and
1012 flavonoid accumulation in Brassica napus in the presence of ultraviolet B radiation.
1013 Photochem Photobiol 84:1445-1454.
1014 Gervasi DD, Schiestl FP. 2017. Real-time divergent evolution in plants driven by pollinators.
1015 Nat Commun 8: 14691.
1016 Gilding EK, Marks MD. 2010. Analysis of purified glabra3-shapeshifter trichomes reveals a role
1017 for NOECK in regulating early trichome morphogenic events. Plant J 64:304-317.
1018 Gómez-Mena C, De Folter S, Costa MMR, Angenent GC, Sablowski R. 2005. Transcriptional
1019 program controlled by the floral homeotic gene AGAMOUS during early organogenesis.
1020 Development 132:429-438.
1021 Goto K, Meyerowitz EM. 1994. Function and regulation of the Arabidopsis floral homeotic gene
1022 PISTILLATA. Gene Dev 8:1548-1560.
1023 Grabherr MG, Haas BJ, Yassour M, Levin JZ, Thompson DA, Amit I, Adiconis X, Fan L,
1024 Raychowdhury R, Zeng Q, Chen Z. 2011. Trinity: reconstructing a full-length
1025 transcriptome without a genome from RNA-Seq data. Nat Biotechnol 29:644.
1026 Grotewold E. 2006. The genetics and biochemistry of floral pigments. Annu Rev Plant Biol
1027 57:761-780.
1028 Guillerme T, Healy K. 2014. mulTree: a package for running MCMCglmm analysis on multiple
1029 trees. ZENODO. 10.5281/zenodo.12902.
1030 Hahn MW, Kern AD. 2004. Comparative genomics of centrality and essentiality in three
1031 eukaryotic protein-interaction networks. Mol Biol Evol 22:803-806.
1032 Haas BJ, Papanicolaou A, Yassour M, Grabherr M, Blood PD, Bowden J, Couger MB, Eccles D,
1033 Li B, Lieber M, MacManes MD. 2013. De novo transcript sequence reconstruction from
1034 RNA-seq using the Trinity platform for reference generation and analysis. Nat Protoc
1035 8:1494.
1036 Hadfield JD. 2010. MCMC methods for multi-response generalized linear mixed models: the
1037 MCMCglmm R pckage. J Stat Softw 33:1-22.

1038 Hermann K, Klahre U, Venail J, Brandenburg A, Kuhlemeier C. 2015. The genetics of
1039 reproductive organ morphology in two Petunia species with contrasting pollination
1040 syndromes. Planta 241:1241-1254.
1041 Hoballah ME, Gübitz T, Stuurman J, Broger L, Barone M, Mandel T, Dell'Olivo A, Arnold M,
1042 Kuhlemeier C. 2007. Single gene-mediated shift in pollinator attraction in Petunia. Plant
1043 Cell 19: 779-790.
1044 Hollender CA, Kang C, Darwish O, Geretz A, Matthews BF, Slovin J, Alkharouf N, Liu Z. 2014.
1045 Floral transcriptomes in woodland strawberry uncover developing receptacle and anther
1046 gene networks. Plant Physiol 165:1062-1075.
1047 Hornett EA, Wheat CW. 2012. Quantitative RNA-Seq analysis in non-model species: assessing
1048 transcriptome assemblies as a scaffold and the utility of evolutionary divergent genomic
1049 reference species. BMC Genomics 13:361.
1050 Horvath S, Dong J. 2008. Geometric interpretation of gene co-expression network analysis.
1051 PLOS Comput Biol 4:e1000117.
1052 Howarth DG, Martins T, Chimney E, Donoghue MJ. 2011. Diversification of CYCLOIDEA
1053 expression in the evolution of bilateral flower symmetry in Caprifoliaceae and *Lonicera*
1054 (Dipsacales). Ann Bot-London 107:1521-1532.
1055 Hu G, Hovav R, Grover CE, Faigenboim-Doron A, Kadmon N, Page JT, Udall JA, Wendel JF.
1056 2016. Evolutionary conservation and divergence of gene coexpression networks in
1057 Gossypium (cotton) seeds. Genome Biol Evol 8:3765-3783.
1058 Hugueney P, Provenzano S, Verriès C, Ferrandino A, Meudec E, Batelli G, Merdinoglu D,
1059 Cheynier V, Schubert A, Ageorges A. 2009. A novel cation-dependent O-
1060 methyltransferase involved in anthocyanin methylation in grapevine. Plant Physiol
1061 150:2057-2070.
1062 Ichihashi Y, Aguilar-Martínez JA, Farhi M, Chitwood DH, Kumar R, Millon LV, Peng J, Maloof
1063 JN, Sinha NR. 2014. Evolutionary developmental transcriptomics reveals a gene network
1064 module regulating interspecific diversity in plant leaf shape. P Natl Acad Sci USA
1065 111:E2616-E2621.
1066 Iorizzo M, Ellison S, Senalik D, Zeng P, Satapoomin P, Huang J, Bowman M, Iovene M,
1067 Sanseverino W, Cavagnaro P, Yildiz M. 2016. A high-quality carrot genome assembly
1068 provides new insights into carotenoid accumulation and asterid genome evolution. Nat
1069 Genet 48:657.
1070 Josephs EB, Wright SI, Stinchcombe JR, Schoen DJ. 2017. The relationship between selection,
1071 network connectivity, and regulatory variation within a population of *Capsella*
1072 *grandiflora*. Genome Biol Evol 9:1099-1109.
1073 Katoh K, Standley DM. 2013. MAFFT multiple sequence alignment software version 7:
1074 improvements in performance and usability. Mol Biol Evol 30:772-780.
1075 Katzer AM, Wessinger CA, Hileman LC. 2019. Nectary size is a pollination syndrome trait in
1076 Penstemon. New Phytol 223:377-384.

1077 Kapralov MV, Votintseva AA, Filatov DA. 2013. Molecular adaptation during a rapid adaptive
1078 radiation. Mol Biol Evol 30:1051-1059.
1079 Kevan PG, Baker HG. 1983. Insects as flower visitors and pollinators. Annu Rev Entomol
1080 28:407-453.
1081 Krylov DM, Wolf YI, Rogozin IB, Koonin EV. 2003. Gene loss, protein sequence divergence,
1082 gene dispensability, expression level, and interactivity are correlated in eukaryotic
1083 evolution. Genome Res 13:2229-2235.
1084 Langfelder P, Horvath S. 2008. WGCNA: an R package for weighted correlation network
1085 analysis. BMC Bioinformatics 9:559.
1086 Langfelder P, Luo R, Oldham MC, Horvath S. 2011. Is my network module preserved and
1087 reproducible? PLOS Comput Biol 7:e1001057.
1088 Laux T, Mayer KF, Berger J, Jurgens G. 1996. The WUSCHEL gene is required for shoot and
1089 floral meristem integrity in Arabidopsis. Development 122:87-96.
1090 Lemos B, Bettencourt BR, Meiklejohn CD, Hartl DL. 2005. Evolution of proteins and gene
1091 expression levels are coupled in *Drosophila* and are independently associated with
1092 mRNA abundance, protein length, and number of protein-protein interactions. Mol Biol
1093 Evol 22:1345-1354.
1094 Li W, Godzik A. 2006. Cd-hit: a fast program for clustering and comparing large sets of protein
1095 or nucleotide sequences. Bioinformatics 22:1658-1659.
1096 Lohmann JU, Hong RL, Hobe M, Busch MA, Parcy F, Simon R, Weigel D. 2001. A molecular
1097 link between stem cell regulation and floral patterning in Arabidopsis. Cell 105:793-803.
1098 Love MI, Huber W, Anders S. 2014. Moderated estimation of fold change and dispersion for
1099 RNA-seq data with DESeq2. Genome Biol 15:550.
1100 Luisi P, Alvarez-Ponce D, Pybus M, Fares MA, Bertranpetit J, Laayouni H. 2015. Recent
1101 positive selection has acted on genes encoding proteins with more interactions within the
1102 whole human interactome. Genome Biol Evol 7:1141-1154.
1103 Luo D, Carpenter R, Copsey L, Vincent C, Clark J, Coen E. 1996. Control of organ asymmetry
1104 in flowers of Antirrhinum. Cell 99:367-376.
1105 Ma X, Zhao H, Xu W, You Q, Yan H, Gao Z, Su Z. 2018. Co-expression gene network analysis
1106 and functional module identification in bamboo growth and development. Front Genetics
1107 9:574.
1108 Mähler N, Wang J, Terebieniec BK, Ingvarsson PK, Street NR, Hvidsten TR. 2017. Gene co-
1109 expression network connectivity is an important determinant of selective constraint.
1110 PLOS Genet 13:e1006402.
1111 Martén-Rodríguez S, Quesada M, Castrao AA, Lopezaraiza-Mikel M, Fenster CB. 2015. A
1112 comparison of reproductive strategies between island and mainland Caribbean
1113 Gesneriaceae. J Ecol 103:1190-1204.
1114 Masalia RR, Bewick AJ, Burke JM. 2017. Connectivity in gene coexpression networks
1115 negatively correlates with rates of molecular evolution in flowering plants. PLOS One
1116 12:e182289.

1117 Mason MJ, Fan G, Plath K, Zhou Q, Horvath S. 2009. Signed weighted gene co-expression
1118 network analysis of transcriptional regulation in murine embryonic stem cells. BMC
1119 Genomics 10:327.
1120 Mayer KF, Schoof H, Haecker A, Lenhard M, Jürgens G, Laux T. 1998. Role of WUSCHEL in
1121 regulating stem cell fate in the Arabidopsis shoot meristem. Cell 95:805-815.
1122 Morandin C, Tin MM, Abril S, Gómez C, Pontieri L, Schiøtt M, Sundström L, Tsuji K, Pedersen
1123 JS, Helanterä H, Mikheyev AS. 2016. Comparative transcriptomics reveals the conserved
1124 building blocks involved in parallel evolution of diverse phenotypic traits in ants.
1125 Genome Biol 17:43.
1126 Morel P, Heijmans K, Ament K, Chopy M, Trehin C, Chambrier P, Bento SR, Bimbo A,
1127 Vandenbussche M. 2018. The floral C-lineage genes trigger nectary development in
1128 Petunia and Arabidopsis. Plant Cell 30:2020-2037.
1129 Nag A, King S, Jack T. 2009. miR319a targeting of TCP4 is critical for petal growth and
1130 development in Arabidopsis. P Natl Acad Sci USA 106:22534-22539.
1131 Neuman H, Galpaz N, Cunningham Jr, FX, Zamir D, Hirschberg J. 2014. The tomato mutation
1132 nxd1 reveals a gene necessary for neoxanthin biosynthesis and demonstrates that
1133 violaxanthin is a sufficient precursor for abscisic acid biosynthesis. Plant J 78:80-93.
1134 Noda KI, Glover BJ, Linstead P, Martin C. 1994. Flower colour intensity depends on specialized
1135 cell shape controlled by a Myb-related transcription factor. Nature 369:661-664.
1136 O'Meara BC, Smith SD, Armbruster WS, Harder LD, Hardy CR, Hileman LC, Hufford L, Litt
1137 A, Magallón S, Smith SA, Stevens PF. 2016. Non-equilibrium dynamics and floral trait
1138 interactions shape extant angiosperm diversity. P Roy Soc B-Biol Sci 283:20152304.
1139 Papiorek S, Junker RR, Alves-dos-Santos I, Melo GA, Amaral-Neto LP, Sazima M, Wolowski
1140 M, Freitas L, Lunau K. 2016. Bees, birds and yellow flowers: pollinator-dependent
1141 convergent evolution of UV patterns. Plant Biol 18:46-55.
1142 Paradis E, Claude J, Strimmer K. 2004. APE: analyses of phylogenetics and evolution in R
1143 language. Bioinformatics 20:289-290.
1144 Parry AD, Horgan R. 1991. Carotenoids and abscisic acid (ABA) biosynthesis in higher plants.
1145 Physiol Plantarum 82:320-326.
1146 Parsana P, Ruberman C, Jaffe AE, Schatz MC, Battle A, Leek JT. 2019. Addressing confounding
1147 artifacts in reconstruction of gene co-expression networks. Genome Biol 20:94.
1148 Patterson AH, Bowers JE, Ruggmann R, Dubchak I, Grimwood J, Gundlach H, Haberer G,
1149 Hellsten U, Mitros T, Poliakov A, Schmutz J. 2009. The *Sorghum bicolor* genome and
1150 the diversification of grasses. Nature 457:551.
1151 Pease JB, Haak DC, Hahn MW, Moyle LC. 2016. Phylogenomics reveals three sources of
1152 adaptive variation during a rapid radiation. PLOS Biol 14:e1002379.
1153 Perret M, Chautems A, Spichiger R, Peixoto M, Savolainen V. 2001. Nectar sugar composition
1154 in relation to pollination syndromes in Sinningieae (Gesneriaceae). Ann Bot-London
1155 87:267-273.

1156 Piechowski D, Dötterl S, Gottsberger G. 2010. Pollination biology and floral scent chemistry of
1157 the Neotropical chieropterophilous Parkia pendula. Plant Biol 12:172-182.
1158 Pickrell JK, Marioni JC, Pai AA, Degner JF, Engelhardt BE, Nkadori E, Veyrieras JB, Stephens
1159 M, Gilad Y, Pritchard JK. 2010. Understanding mechanisms underlying human gene
1160 expression variation with RNA sequencing. Nature 464:768.
1161 Pollastri S, Tattini M. 2011. Flavonols: old compounds for old roles. Ann Bot-London 108:1225-
1162 1233.
1163 Prasad A, Kumar SS, Dessimoz C, Bleuler S, Laule O, Hruz T, Gruissem W, Zimmerman P.
1164 2013. Global regulatory architecture of human, mouse and rat tissue transcriptomes.
1165 BMC Genomics 14:716.
1166 Preston JC, Hileman LC, Cubas P. 2011. Reduce, reuse, and recycle: developmental evolution of
1167 trait diversification. Am J Bot 98:397-403.
1168 Preston JC, Martinez CC. Hileman LC. 2011. Gradual disintegration of the floral symmetry gene
1169 network is implicated in the evolution of a wind-pollination syndrome. P Natl Acad Sci
1170 USA 108:2343-2348.
1171 Price MN, Dehal PS, Arkin AP. 2010. FastTree 2—approximately maximum-likelihood trees for
1172 large alignments. PLOS One 5:e9490.
1173 Provenzano S, Spelt C, Hosokawa S, Nakamura N, Brugliera F, Demelis L, Geerke DP, Schubert
1174 A, Tanaka Y, Quattrocchio F, Koes R. 2014. Genetic control and evolution of
1175 anthocyanin methylation. Plant Physiol 165:962-977.
1176 Quattrocchio F, Wing J, van der Woude K, Souer E, de Vetten N, Mol J, Koes R. 1999.
1177 Molecular analysis of the *anthocyanin2* gene of petunia and its role in the evolution of
1178 flower color. Plant Cell 11:1433-1444.
1179 Raherison ESM, Giguère I, Caron S, Lamara M, MacKay JJ. 2015. Modular organization of the
1180 white spruce (*Picea glauca*) transcriptome reveals functional organization and
1181 evolutionary signatures. New Phytol 207:172-187.
1182 Ramírez-Aguirre E, Martén-Rodríguez S, Quesada-Avila G, Quesada M, Martínez-Díaz Y,
1183 Oyama K, Espinosa-García FJ. 2019. Reproductive isolation among three sympatric
1184 *Achimenes* species: pre- and post-pollination components. Am J Bot 106:1021-1031.
1185 Ramírez Roa MA. 1987. Revision de *Achimenes* (Gesneriaceae). PhD dissertation, Universidad
1186 Nacional Autonoma de Mexico, Mexico City, Mexico.
1187 Ravasz E, Somera AL, Mongru DA, Oltvai ZN, Barbási AL. 2002. Hierarchical organization of
1188 modularity in metabolic networks. Science 297:1551-1555.
1189 Rice-Evans CA, Miller N, Papanga G. 1996. Structure-antioxidant relationships of flavonoids
1190 and phenolic acids. Free Radical Bio Med 20:933-956.
1191 Ritchie W, Rajasekhar M, Flamant S, Rasko JE. 2009. Conserved expression patterns predict
1192 microRNA targets. PLOS Comput Biol 5:e1000513.
1193 Roalson EH, Roberts WR. 2016. Distinct processes drive diversification in different clades of
1194 Gesneriaceae. Syst Biol 65:662-684.

1195 Roalson EH, Skog LE, Zimmer EA. 2003. Phylogenetic relationships and the diversification of
1196 floral form in *Achimenes* (Gesneriaceae). Syst Bot 28:593-608.
1197 Roberts WR, Roalson EH, 2017. Comparative transcriptome analyses of flower development in
1198 four species of *Achimenes* (Gesneriaceae). BMC Genomics 18:240.
1199 Roberts WR, Roalson EH. 2018. Phylogenomic analyses reveal extensive gene flow within the
1200 magic flowers (*Achimenes*). Am J Bot 105:726-740.
1201 Romero IG, Ruvinsky I, Gilad Y. 2012. Comparative studies of gene expression and the
1202 evolution of gene regulation. Nat Rev Genet 13:505-516.
1203 Ronen G, Carmel-Goren L, Zamir D, Hirschberg J. 2000. An alternative pathway to β-carotene
1204 formation in plant chromoplasts discovered by map-based cloning of Beta and old-gold
1205 color mutations in tomato. P Natl Acad Sci USA 97:11102-11107.
1206 Rosas-Guerrero V, Aguilar R, Martén-Rodriguez S, Ashworth L, Lopezaraiza-Mikel M, Bastida
1207 JM, Quesada M. 2014. A quantitative review of pollination syndromes: do floral traits
1208 predict effective pollinators? Ecol Lett 17:388-400.
1209 Rosas-Saavedra C, Stange C. 2016. Biosynthesis of carotenoids in plants: Enzymes and color. In:
1210 Stange C, editor. *Carotenoids in nature: biosynthesis, regulation and function*. Vol. 79.
1211 Springer. p. 35-69.
1212 Saito K, Yamazaki M. 2002. Biochemistry and molecular biology of the late-stage of
1213 biosynthesis of anthocyanin: lessons from Perilla frutescens as a model plant. New Phytol
1214 155:9-23.
1215 Sakata Y, Aoki N, Tsunematsu S, Nishikouri H, Johjima T. 1995. Petal coloration and
1216 pigmentation of tree peony bred and selected in Daikon island (Shimane Prefecture). J
1217 Jpn Soc Hortic Sci 65:351-357.
1218 Sauquet H, Magallón S. 2018. Key questions and challenges in angiosperm macroevolution.
1219 New Phytol 219:1170-1187.
1220 Scoville AG, Barnett LL, Bodbyl-Roels S, Kelly JK, Hileman LC. 2011. Differential regulation
1221 of a MYB transcription factor is correlated with transgenerational epigenetic inheritance
1222 of trichome density in Mimulus guttatus. New Phytol 191:251-263.
1223 Serrano-Serrano ML, Marcionetti A, Perret M, Salamin N. 2017a. Transcriptome resources for
1224 an endemic Neotropical plant lineage (Gesneriaceae). Appl Plant Sci 5:1600135.
1225 Serrano-Serrano ML, Rolland J, Clark JL, Salamin N, Perret M. 2017b. Hummingbird
1226 pollination and the diversification of angiosperms: an old and successful association in
1227 Gesneriaceae. P Roy Soc B-Biol Sci 284:20162816.
1228 Shahan R, Zawora C, Wight H, Sittmann J, Wang W, Mount SM, Liu Z. 2018. Consensus
1229 coexpression network analysis identifies key regulators of flower and fruit development
1230 in wild strawberry. Plant Physiol 178:202-216.
1231 Simão FA, Waterhouse RM, Ioannidis P, Kriventseva EV, Zbodnov EM. 2015. BUSCO:
1232 assessing genome assembly and annotation completeness with single-copy orthologs.
1233 Bioinformatics 31:3210-3212.

1234 Sletvold N, Grindeland JM, Ågren J. 2010. Pollinator-mediated selection on floral display, spur
1235 length and flowering phenology in the deceptive orchid Dactylorhiza lapponica. New
1236 Phytol 188:385-392.
1237 Sletvold N, Trunschke J, Smit M, Verbeek J, Ågren J. 2016. Strong pollinator-mediated selection
1238 for increased flower brightness and contrast in a deceptive orchid. Evolution 70:716-724.
1239 Smith SA, Dunn CW. 2008. Phyutility: a phyloinformatics tool for trees, alignments and
1240 molecular data. Bioinformatics 24:715-716.
1241 Smith SD, Rausher MD. 2011. Gene loss and parallel evolution contribute to species difference
1242 in flower color. Mol Biol Evol 28:2799-2810.
1243 Smith SD, Wang S, Rausher MD. 2013. Functional evolution of an anthocyanin pathway enzyme
1244 during a flower color transition. Mol Biol Evol 30:602-612.
1245 Song L, Langfelder P, Horvath S. 2012. Comparison of co-expression measures: mutual
1246 information, correlation, and model based indices. BMC Bioinformatics 13:328.
1247 Springob K. Nakajima JI, Yamazaki M, Saito K. 2003. Recent advances in the biosynthesis and
1248 accumulation of anthocyanins. Nat Prod Rep 20:288-303.
1249 Stamatakis A. 2014. RAxML version 8: a tool for phylogenetic analysis and post-analysis of
1250 large phylogenies. Bioinformatics 30:1312-1313.
1251 Stebbins GL. 1970. Adaptive radiation of reproductive characteristics in angiosperms, I:
1252 pollination mechanisms. Annu Rev Ecol Syst 1:307-326.
1253 Sun B, Xu Y, Ng KH, Ito T. 2009. A timing mechanism for stem cell maintenance and
1254 differentiation in the Arabidopsis floral meristem. Gene Dev 23:1791-1804.
1255 Supek F, Bošnjak M, Škunca N, Šmuc T. 2011. REVIGO summarizes and visualizes long lists of
1256 gene ontology terms. PLOS One 6:e21800.
1257 Suyama M, Torrents D, Bork P. 2006. PAL2NAL: robust conversion of protein sequence
1258 alignments into the corresponding codon alignments. Nucleic Acids Res 34:W609-W612.
1259 Suzuki JY, Amore TD, Calla B, Palmer NA, Scully ED, Sattler SE, Sarath G, Lichty JS, Myers
1260 RY, Keith LM, Matsumoto TK. 2017. Organ-specific transcriptome profiling of
1261 metabolic and pigment biosynthetic pathways in the floral ornamental progenitor species
1262 *Anthurium amnicola* Dressler. Sci Rep-UK 7:1596.
1263 Tahara S. 2007. A journey of twenty-five years through the ecological biochemistry of
1264 flavonoids. Biosci Biotechnol Biochem 71:1387-1404.
1265 Tanaka Y, Sasaki N, Ohmiya A. 2008. Biosynthesis of plant pigments: anthocyanins, betalains
1266 and carotenoids. Plant J 54:733-749.
1267 Tang H, Wang X, Bowers JE, Ming R, Alam M, Paterson AH. 2008. Unraveling ancient
1268 hexaploidy through multiply-aligned angiosperm gene maps. Genome Res 18:1944-1954.
1269 Tröbner W, Ramirez L, Motte P, Hue I, Huijser P, Löning WE, Saedler H, Sommer H, Schwarz-
1270 Sommer Z. 1992. GLOBOSA: a homeotic gene which interacts with DEFICIENS in the
1271 control of Antirrhinum floral organogenesis. EMBO J 11:4693-4704.

1272 Uebbing S, Künster A, Mäkinen H, Backström N, Bolivar P, Burri R, Dutoit L, Mugal CF, Nater
1273 A, Aken B, Flicek P. 2016. Divergence in gene expression within and between two
1274 closely related flycatcher species. Mol Ecol 25:2015-2028.
1275 The UniProt Consortium. 2017. UniProt: the universal protein knowledgebase. Nucleic Acids
1276 Res 45:D158-D169.
1277 Van Dam S, Võsa U, van der Graaf A, Franke L, de Magalhaes JP. 2018. Gene co-expression
1278 analysis for functional classification and gene-disease predictions. Brief Bioinform
1279 19:575-592.
1280 Vandelook F, Janssens SB, Gijbels P, Fischer E, Van den Ende W, Honnay O, Abrahamczyk S.
1281 2019. Nectar traits differ between pollination syndromes in Balsaminaceae. Ann Bot-
1282 London 124:269-279.
1283 Van der Niet T, Johnson SD. 2012. Phylogenetic evidence for pollinator-driven diversification of
1284 angiosperms. Trends Ecol Evol 27: 353-361.
1285 Vincent CA, Enrico SC. 2004. A temporal and morphological framework for flower
1286 development in Antirrhinum majus. Can J Botany 82:681-690.
1287 Waites R, Selvadurai HR, Oliver IR, Hudson A. 1998. The PHANTASTICA gene encodes a
1288 MYB transcription factor involved in growth and dorsoventrality of lateral organs in
1289 Antirrhinum. Cell 93:779-789.
1290 Wang M, Wang G, Ji J, Wang J. 2009. The effect of pds gene silencing on chloroplast pigment
1291 composition, thylakoid membrane structure and photosynthesis efficiency in tobacco
1292 plants. Plant Sci 177:222-226.
1293 Wessinger CA, Rausher MD. 2014. Ecological transition predictably associated with gene
1294 degeneration. Mol Biol Evol 32:347-354.
1295 West-Eberhard MJ. 1989. Phenotypic plasticity and the origins of diversity. Ann Rev Ecol Syst
1296 20:249-278.
1297 Whitney HM, Glover BJ, Walker R, Ellis AG. 2011. The contribution of epidermal structure to
1298 flower colour in the South African flora. Curtis's Botanical Magazine 28:349-371.
1299 Wiehler H. 1983. A synopsis of the neotropical Gesneriaceae. Selbyana 6:1-219.
1300 Winkel-Shirley B. 2002. Biosynthesis of flavonoids and effects of stress. Curr Opinion Plant
1301 Biol 5:218-223.
1302 Wu CA, Streisfeld MA, Nutter LI, Cross KA. 2013. The genetic basis of a rare flower color
1303 polymorphism in Mimulus lewisii provides insight into the repeatability of evolution.
1304 PLOS One 8:12.
1305 Yang Y, Smith SA. 2014. Orthology inference in nonmodel organisms using transcriptomes and
1306 low-coverage genomes: improving accuracy and matrix occupancy for phylogenomics.
1307 Mol Biol Evol 31:3081-3092.
1308 Yang Z. 2007. PAML 4: phylogenetic analysis by maximum likelihood. Mol Biol Evol 24:1586-
1309 1591.
1310 Yant L, Collani S, Puzey J, Levy C, Kramer EM. 2015. Molecular basis for three-dimensional
1311 elaboration of the Aquilegia petal spur. P Roy Soc B-Biol Sci 282:20142778.

1312 Yuan YW, Rebocho AB, Sagawa JM, Stanley LE, Bradshaw HD. 2016. Competition between
1313 anthocyanin and flavonol biosynthesis produces spatial pattern variation of floral
1314 pigments between Mimulus species. P Natl Acad Sci USA 113: 2448-2453.
1315 Yuan YW, Sagawa JM, Young RC, Christensen BJ, Bradshaw HD. 2013. Genetic dissection of a
1316 major anthocyanin QTL contributing to pollinator-mediated reproductive isolation
1317 between sister species of Mimulus. Genetics 194:255-263.
1318 Zhang JS, Li Z, Zhao J, Zhang S, Quan H, Zhao H, He C. 2014. Deciphering the Physalis
1319 floridana double-layered-lantern1 mutant provides insights into the functional divergence
1320 of the GLOBOSA duplicates within the Solanaceae. Plant Physiol 164:748-764.
1321 Zhang W, Kramer EM, Davis CC. 2010. Floral symmetry genes and the origin and maintenance
1322 of zygomorphy in a plant-pollinator mutualism. P Natl Acad Sci USA 107:6388-6393.
1323 Zhou XR, Wang YZ, Smith JF, Chen R. 2008. Altered expression patterns of TCP and MYB
1324 genes relating to the floral developmental transition from initial zygomorphy to
1325 actinomorphy in Bournea (Gesneriaceae). New Phytol 178:532-543.
1326 Zuo J, Niu Q-W, Frugis G, Chua N-H. 2002. The WUSCHEL gene promotes vegetative-to-
1327 embryonic transition in Arabidopsis. Plant J 30:349-359.
1328

Tables

Table 1. Definition of pollination syndromes in *Achimenes, Eucodonia,* and *Gesneria*.

Table 2. Gene Ontology enrichment for the network hubs.

Table 3. Gene Ontology enrichment for the network periphery.

Table 4. Gene Ontology enrichment in Bud stage modules correlated to pollination syndrome.

Table 5. Gene Ontology enrichment in D stage modules correlated to pollination syndrome.

Figures

Figure 1. *Achimenes* flowers and the sampled developmental stages. Flowers of the twelve sampled species: (A) *A. admirabilis,* (B) *A. antirrhina,* (C) *A. candida*, (D) *A. cettoana,* (E) *A. erecta,* (F) *A. grandiflora,* (G) *A. longiflora,* (H) *A. misera,* (I) *A. patens,* (J) *A. pedunculate,* (K) *E. verticillate,* and (L) *G. cuneifolia*. Sampled Bud and D stage flowers for (M-N) *A. cettoana,* (O-P) *A. erecta,* (Q-R) *A. misera,* and (S-T) *A. patens*. Corolla spurs found in (U) *A. grandiflora* and (V) *A. patens* are indicated with arrows. Scale bars equal 1 cm. Abbreviations: A, *Achimenes*; E, *Eucodonia*; G, *Gesneria*.

Figure 2. Phylogenetic relationships and floral traits in *Achimenes*. Phylogeny of *Achimenes* adapted from Roberts and Roalson (2018). Clade 1 and Clade 2 (sensu Roalson et al. 2003) are indicated on the phylogeny with a circle and box, respectively. Flower traits for each species are shown at the tips of the phylogeny, including flower color, flower shape, presence of corolla spurs, pollination syndrome, and pollinator observations.

Figure 3. Co-expression clustering of the Bud and D stages. Hierarchical clustering by WGCNA showing co-expressed modules for (A) the Bud Stage and (B) the D stage. Each of the 9503 orthogroups were assigned to 65 and 62 modules, respectively, and the color rows underneath show the module assignment.

Figure 4. Correspondence of the Bud and D stage networks. Each row corresponds to one Bud stage module (labeled by module name and module size), and each column corresponds to one D stage module (labeled by module name and module size). Numbers in the table indicate gene counts in the intersection of the corresponding modules. Coloring of the table encodes -log(p), with p being the Fisher's exact test p-value for the overlap of the two modules. The stronger the red color, the more significant the overlap.

Figure 5. Summary of Bud stage network module association to floral traits and pollination syndrome. Each row represents an individual module in the Bud stage network and shows the total size (column All), the number of hubs (column Hubs), and whether the module is preserved in the D stage. Each column in the central table represents the floral traits (Pollination Syndrome,

Flower Color, Flower Shape, and Spurs) that were tested for an association to module eigengenes using MCMCglmm. The eigengene expression is indicated for each module in which all three replicates from an individual species had > 1.0 or < -1.0 expression. An association was considered strong when both MCMCglmm results were significant and the eigengene expression was > 1.0 or < -1.0 in multiple species that shared the significant trait. An association was considered weak when MCMCglmm results were significant but the eigengene was > 1.0 or < -1.0 in a single species or no species that shared the significant trait. Eigengene expression for species that share traits to those found significant by MCMCglmm are in bold.

Figure 6. Summary of D stage network module association to floral traits and pollination syndrome. Each row represents an individual module in the D stage network and shows the total size (column All), the number of hubs (column Hubs), and whether the module is preserved in the Bud stage. Each column in the central table represents the floral traits (Pollination Syndrome, Flower Color, Flower Shape, and Spurs) that were tested for an association to module eigengenes using MCMCglmm. The eigengene expression is indicated for each module in which all three replicates from an individual species had > 1.0 or < -1.0 expression. An association was considered strong when both MCMCglmm results were significant and the eigengene expression was > 1.0 or < -1.0 in multiple species that shared the significant trait. An association was considered weak when MCMCglmm results were significant but the eigengene was > 1.0 or < -1.0 in a single species or no species that shared the significant trait. Eigengene expression for species that share traits to those found significant by MCMCglmm are in bold.

Figure 7. Relationship between orthogroup dN/dS (omega) and orthogroup connectivity. (A) Bud stage network. (B) D stage network. Each point represents an individual orthogroup. The red line indicates the linear regression line for the relationship between dN/dS and connectivity. The dotted line indicates dN/dS = 1 with orthogroups above this line considered to be under relaxed or positive selection.

Table 1. Definition of pollination syndromes in *Achimenes, Eucodonia*, and *Gesneria*.

Pollination syndrome	Primary flower color	Flower shape	Presence of corolla spurs	Species
Melittophily (bees)	White or Purple with yellow or purple spotted throat	Funnelform	No	*Achimenes candida*
				Achimenes misera
				Eucodonia verticillata
Ornithophily (hummingbirds)	Red and yellow	Tubular, Salverform	No	*Achimenes admirabilis*
				Achimenes antirrhina
				Achimenes erecta
				Achimenes pedunculata
				Gesneria cuneifolia
Psychophily (butterflies)	Purple	Salverform	Yes	*Achimenes cettoana*
				Achimenes grandiflora
				Achimenes longiflora
				Achimenes patens

Table 2. Gene Ontology enrichment for the network hubs.

	GO ID	Term	Annotated	Significant	Expected	P
A. Bud stage Hubs	GO:0031325	positive regulation of cellular metabolic process	224	16	14.52	0.000
	GO:0006607	NLS-bearing protein import into nucleus	7	4	0.45	0.001
	GO:0015991	ATP hydrolysis coupled proton transport	9	4	0.58	0.002
	GO:0046470	phosphatidylcholine metabolic process	9	4	0.58	0.002
	GO:0018298	protein-chromophore linkage	32	7	2.07	0.004
	GO:0070507	regulation of microtubule cytoskeleton organization	6	3	0.39	0.005
	GO:1990778	protein localization to cell periphery	6	3	0.39	0.005
	GO:0051592	response to calcium ion	7	3	0.45	0.008
	GO:0006412	translation	233	24	15.10	0.009
	GO:0042594	response to starvation	60	10	3.89	0.012
	GO:0007035	vacuolar acidification	8	3	0.52	0.012
	GO:0006534	cysteine metabolic process	9	4	0.58	0.012
	GO:0009833	plant-type primary cell wall biogenesis	15	4	0.97	0.013
	GO:0048831	regulation of shoot system development	123	12	7.97	0.017
	GO:0032509	endosome transport via multivesicular body sorting pathway	9	3	0.58	0.017
	GO:0051568	histone H3-K4 methylation	9	3	0.58	0.017
	GO:0000271	polysaccharide biosynthetic process	123	11	7.97	0.023
	GO:0006732	coenzyme metabolic process	116	8	7.52	0.023
	GO:0010338	leaf formation	5	2	0.32	0.037
	GO:0048564	photosystem I assembly	5	2	0.32	0.037
	GO:0017001	antibiotic catabolic process	26	3	1.69	0.037
	GO:0044282	small molecule catabolic process	75	10	4.86	0.038
	GO:0006833	water transport	13	3	0.84	0.048
	GO ID	Term	Annotated	Significant	Expected	P
B. D stage Hubs	GO:0006412	translation	233	30	16.03	0.001
	GO:0042939	tripeptide transport	8	4	0.55	0.001
	GO:0016117	carotenoid biosynthetic process	20	6	1.38	0.002
	GO:0006744	ubiquinone biosynthetic process	5	3	0.34	0.003
	GO:0032259	methylation	88	15	6.05	0.004
	GO:0045814	negative regulation of gene expression, epigenetic	37	5	2.55	0.005
	GO:0009206	purine ribonucleoside triphosphate biosynthetic process	44	6	3.03	0.013
	GO:0000271	polysaccharide biosynthetic process	123	11	8.46	0.013
	GO:0009873	ethylene-activated signaling pathway	78	12	5.37	0.014
	GO:0015991	ATP hydrolysis coupled proton transport	9	3	0.62	0.020
	GO:0009718	anthocyanin-containing compound biosynthetic process	26	5	1.79	0.030
	GO:0000018	regulation of DNA recombination	5	2	0.34	0.041
	GO:0015976	carbon utilization	5	2	0.34	0.041
	GO:0034314	Arp2/3 complex-mediated actin nucleation	5	2	0.34	0.041
	GO:0080144	amino acid homeostasis	5	2	0.34	0.041
	GO:1901615	organic hydroxy compound metabolic process	121	9	8.32	0.041
	GO:0000902	cell morphogenesis	174	9	11.97	0.042

Table 3. Gene Ontology enrichment for the network periphery.

	GO.ID	Term	Annotated	Significant	Expected	P
A. Bud stage periphery	GO:0016579	protein deubiquitination	24	16	8.70	0.002
	GO:0048825	cotyledon development	21	12	7.61	0.005
	GO:0015846	polyamine transport	5	5	1.81	0.006
	GO:0034314	Arp2/3 complex-mediated actin nucleation	5	5	1.81	0.006
	GO:0006020	inositol metabolic process	12	7	4.35	0.011
	GO:0010229	inflorescence development	9	7	3.26	0.014
	GO:0009744	response to sucrose	31	16	11.24	0.021
	GO:1903338	regulation of cell wall organization or biogenesis	11	7	3.99	0.026
	GO:0006809	nitric oxide biosynthetic process	6	5	2.18	0.026
	GO:0009773	photosynthetic electron transport in photosystem I	8	6	2.90	0.030
	GO:0034613	cellular protein localization	183	75	66.34	0.031
	GO:0006004	fucose metabolic process	12	8	4.35	0.032
	GO:0009926	auxin polar transport	42	22	15.23	0.037
	GO:0010090	trichome morphogenesis	38	19	13.78	0.041
	GO:0009414	response to water deprivation	182	69	65.98	0.045
	GO:0009873	ethylene-activated signaling pathway	78	38	28.28	0.046
	GO:0007166	cell surface receptor signaling pathway	93	42	33.71	0.046
	GO:0006163	purine nucleotide metabolic process	96	38	34.80	0.047
	GO:0035195	gene silencing by miRNA	15	7	5.44	0.048
	GO:0016236	macroautophagy	21	9	7.61	0.048
	GO:0055083	monovalent inorganic anion homeostasis	13	5	4.71	0.048
	GO:0051338	regulation of transferase activity	38	13	13.78	0.048
	GO:0006473	protein acetylation	23	7	8.34	0.048
	GO.ID	Term	Annotated	Significant	Expected	P
B. D stage periphery	GO:0045490	pectin catabolic process	20	19	12.88	0.002
	GO:0007166	cell surface receptor signaling pathway	93	71	59.90	0.006
	GO:0000398	mRNA splicing, via spliceosome	46	38	29.63	0.007
	GO:0009740	gibberellic acid mediated signaling pathway	31	24	19.97	0.015
	GO:0006310	DNA recombination	54	41	34.78	0.015
	GO:0009909	regulation of flower development	80	57	51.53	0.017
	GO:0009058	biosynthetic process	2121	1360	1366.19	0.019
	GO:0042545	cell wall modification	34	26	21.90	0.021
	GO:0001708	cell fate specification	13	12	8.37	0.027
	GO:0042538	hyperosmotic salinity response	25	21	16.10	0.027
	GO:0002181	cytoplasmic translation	21	18	13.53	0.029
	GO:0006897	endocytosis	40	27	25.76	0.029
	GO:0010197	polar nucleus fusion	20	17	12.88	0.039
	GO:0071702	organic substance transport	492	319	316.91	0.046
	GO:0006949	syncytium formation	7	7	4.51	0.046
	GO:0008295	spermidine biosynthetic process	7	7	4.51	0.046
	GO:0009963	positive regulation of flavonoid biosynthetic process	7	7	4.51	0.046

Table 4. Gene Ontology enrichment in Bud stage modules correlated to pollination syndrome.

A. Bee pollination

GO.ID	Term	Annotated	Significant	Expected	P
GO:0046686	response to cadmium ion	99	16	5.69	0.000
GO:0010104	regulation of ethylene-activated signaling pathway	12	3	0.69	0.003
GO:0010189	vitamin E biosynthetic process	8	3	0.46	0.008
GO:0070085	glycosylation	72	7	4.13	0.009
GO:0009226	nucleotide-sugar biosynthetic process	21	5	1.21	0.011
GO:0042136	neurotransmitter biosynthetic process	9	4	0.52	0.018
GO:0070592	cell wall polysaccharide biosynthetic process	32	4	1.84	0.018
GO:0051173	positive regulation of nitrogen compound metabolic process	192	4	11.03	0.019
GO:0046777	protein autophosphorylation	71	9	4.08	0.019
GO:0009651	response to salt stress	215	19	12.35	0.022
GO:0009738	abscisic acid-activated signaling pathway	135	11	7.75	0.028
GO:0015718	monocarboxylic acid transport	12	3	0.69	0.028
GO:0046889	positive regulation of lipid biosynthetic process	12	3	0.69	0.029
GO:0006809	nitric oxide biosynthetic process	5	2	0.29	0.029
GO:0006974	cellular response to DNA damage stimulus	99	9	5.69	0.035
GO:0010099	regulation of photomorphogenesis	6	2	0.34	0.042
GO:0071805	potassium ion transmembrane transport	6	2	0.34	0.042

B. Butterfly pollination

GO.ID	Term	Annotated	Significant	Expected	P
GO:0009415	response to water	155	13	11.47	0.016
GO:0008380	RNA splicing	122	16	9.03	0.016
GO:0010223	secondary shoot formation	14	4	1.04	0.016
GO:0009624	response to nematode	15	4	1.11	0.021
GO:0009695	jasmonic acid biosynthetic process	9	3	0.67	0.024
GO:0090691	formation of plant organ boundary	9	3	0.67	0.024
GO:0006950	response to stress	1173	83	86.79	0.028
GO:0006353	DNA-templated transcription, termination	17	4	1.26	0.032
GO:0009567	double fertilization forming a zygote and endosperm	11	3	0.81	0.042
GO:0009835	fruit ripening	11	3	0.81	0.042
GO:0009607	response to biotic stimulus	374	35	27.67	0.045

GO:0010216	maintenance of DNA methylation	5	2	0.37	0.047
GO:0010363	regulation of plant-type hypersensitive response	5	2	0.37	0.047
GO:0071577	zinc ion transmembrane transport	5	2	0.37	0.047
GO:0009825	multidimensional cell growth	19	4	1.41	0.047

C. Hummingbird pollination

GO.ID	Term	Annotated	Significant	Expected	P
GO:0009451	RNA modification	353	89	62.34	0.000
GO:1900618	regulation of shoot system morphogenesis	9	5	1.59	0.001
GO:0009826	unidimensional cell growth	95	24	16.78	0.002
GO:0016556	mRNA modification	35	11	6.18	0.002
GO:0006012	galactose metabolic process	5	4	0.88	0.004
GO:0031425	chloroplast RNA processing	18	8	3.18	0.008
GO:0008643	carbohydrate transport	44	15	7.77	0.010
GO:1905428	regulation of plant organ formation	6	4	1.06	0.011
GO:0006888	ER to Golgi vesicle-mediated transport	19	8	3.36	0.011
GO:0044272	sulfur compound biosynthetic process	58	12	10.24	0.011
GO:0045944	positive regulation of transcription by RNA polymerase II	37	13	6.53	0.013
GO:0002239	response to oomycetes	18	6	3.18	0.019
GO:0006813	potassium ion transport	16	7	2.83	0.020
GO:0043650	dicarboxylic acid biosynthetic process	10	5	1.77	0.020
GO:0051053	negative regulation of DNA metabolic process	7	4	1.24	0.022
GO:0051301	cell division	147	30	25.96	0.027
GO:0000079	regulation of cyclin-dependent protein serine/threonine kinase activity	11	5	1.94	0.031
GO:0046131	pyrimidine ribonucleoside metabolic process	12	3	2.12	0.031
GO:0032509	endosome transport via multivesicular body sorting pathway	8	4	1.41	0.037
GO:0071496	cellular response to external stimulus	71	17	12.54	0.041
GO:1902117	positive regulation of organelle assembly	5	3	0.88	0.041
GO:0048438	floral whorl development	69	12	12.19	0.042
GO:0009651	response to salt stress	215	49	37.97	0.043

Table 5. Gene Ontology enrichment in D stage modules correlated to pollination syndrome.

A. Bee pollination

GO.ID	Term	Annotated	Significant	Expected	P
GO:0061014	positive regulation of mRNA catabolic process	6	3	0.26	0.002
GO:0010189	vitamin E biosynthetic process	8	3	0.35	0.004
GO:0044093	positive regulation of molecular function	46	4	2.01	0.006
GO:0046686	response to cadmium ion	99	10	4.33	0.011
GO:0006974	cellular response to DNA damage stimulus	99	8	4.33	0.017
GO:0002833	positive regulation of response to biotic stimulus	19	3	0.83	0.017
GO:0009395	phospholipid catabolic process	5	2	0.22	0.017
GO:0009969	xyloglucan biosynthetic process	5	2	0.22	0.017
GO:0006544	glycine metabolic process	7	2	0.31	0.035
GO:0043488	regulation of mRNA stability	7	2	0.31	0.035
GO:0016569	covalent chromatin modification	58	4	2.54	0.044
GO:0043902	positive regulation of multi-organism process	22	3	0.96	0.045
GO:0009631	cold acclimation	8	2	0.35	0.045

B. Butterfly pollination

GO.ID	Term	Annotated	Significant	Expected	P
GO:0009853	photorespiration	19	7	2.00	0.002
GO:0043622	cortical microtubule organization	13	5	1.37	0.008
GO:0031349	positive regulation of defense response	51	8	5.37	0.010
GO:0006575	cellular modified amino acid metabolic process	35	7	3.69	0.018
GO:0070919	production of siRNA involved in chromatin silencing by small RNA	6	3	0.63	0.018
GO:0042398	cellular modified amino acid biosynthetic process	7	3	0.74	0.029
GO:0009808	lignin metabolic process	22	5	2.32	0.031
GO:2000030	regulation of response to red or far red light	9	3	0.95	0.031
GO:0019220	regulation of phosphate metabolic process	39	6	4.11	0.031
GO:0010197	polar nucleus fusion	13	4	1.37	0.040
GO:0051028	mRNA transport	44	9	4.63	0.041
GO:0006833	water transport	13	4	1.37	0.043
GO:0043902	positive regulation of multi-organism process	22	4	2.32	0.044

C. Hummingbird pollination

GO.ID	Term	Annotated	Significant	Expected	P

GO:0009960	endosperm development	10	6	1.53	0.002
GO:0007163	establishment or maintenance of cell polarity	5	4	0.77	0.002
GO:0000272	polysaccharide catabolic process	50	14	7.65	0.005
GO:0010224	response to UV-B	24	9	3.67	0.007
GO:0009089	lysine biosynthetic process via diaminopimelate	7	4	1.07	0.013
GO:0009451	RNA modification	353	70	54.01	0.015
GO:0007166	cell surface receptor signaling pathway	86	21	13.16	0.018
GO:0008285	negative regulation of cell proliferation	8	4	1.22	0.023
GO:0042939	tripeptide transport	8	4	1.22	0.023
GO:0009955	adaxial/abaxial pattern specification	17	8	2.60	0.023
GO:0051656	establishment of organelle localization	36	9	5.51	0.023
GO:0006213	pyrimidine nucleoside metabolic process	14	3	2.14	0.023
GO:0033014	tetrapyrrole biosynthetic process	39	6	5.97	0.024
GO:0009267	cellular response to starvation	47	14	7.19	0.025
GO:0006635	fatty acid beta-oxidation	16	6	2.45	0.026
GO:0016556	mRNA modification	35	9	5.36	0.026
GO:0048438	floral whorl development	69	14	10.56	0.028
GO:0010103	stomatal complex morphogenesis	14	5	2.14	0.028
GO:0006383	transcription by RNA polymerase III	5	3	0.77	0.028
GO:0040008	regulation of growth	126	26	19.28	0.029
GO:0010019	chloroplast-nucleus signaling pathway	9	4	1.38	0.036
GO:0010506	regulation of autophagy	9	4	1.38	0.036
GO:0043547	positive regulation of GTPase activity	9	4	1.38	0.036
GO:0018298	protein-chromophore linkage	27	8	4.13	0.044
GO:0031425	chloroplast RNA processing	18	6	2.75	0.045
GO:0051187	cofactor catabolic process	34	9	5.20	0.050
GO:0002238	response to molecule of fungal origin	6	3	0.92	0.050
GO:0032958	inositol phosphate biosynthetic process	6	3	0.92	0.050
GO:0042219	cellular modified amino acid catabolic process	6	3	0.92	0.050
GO:1905428	regulation of plant organ formation	6	3	0.92	0.050
GO:0065004	protein-DNA complex assembly	45	8	6.89	0.050

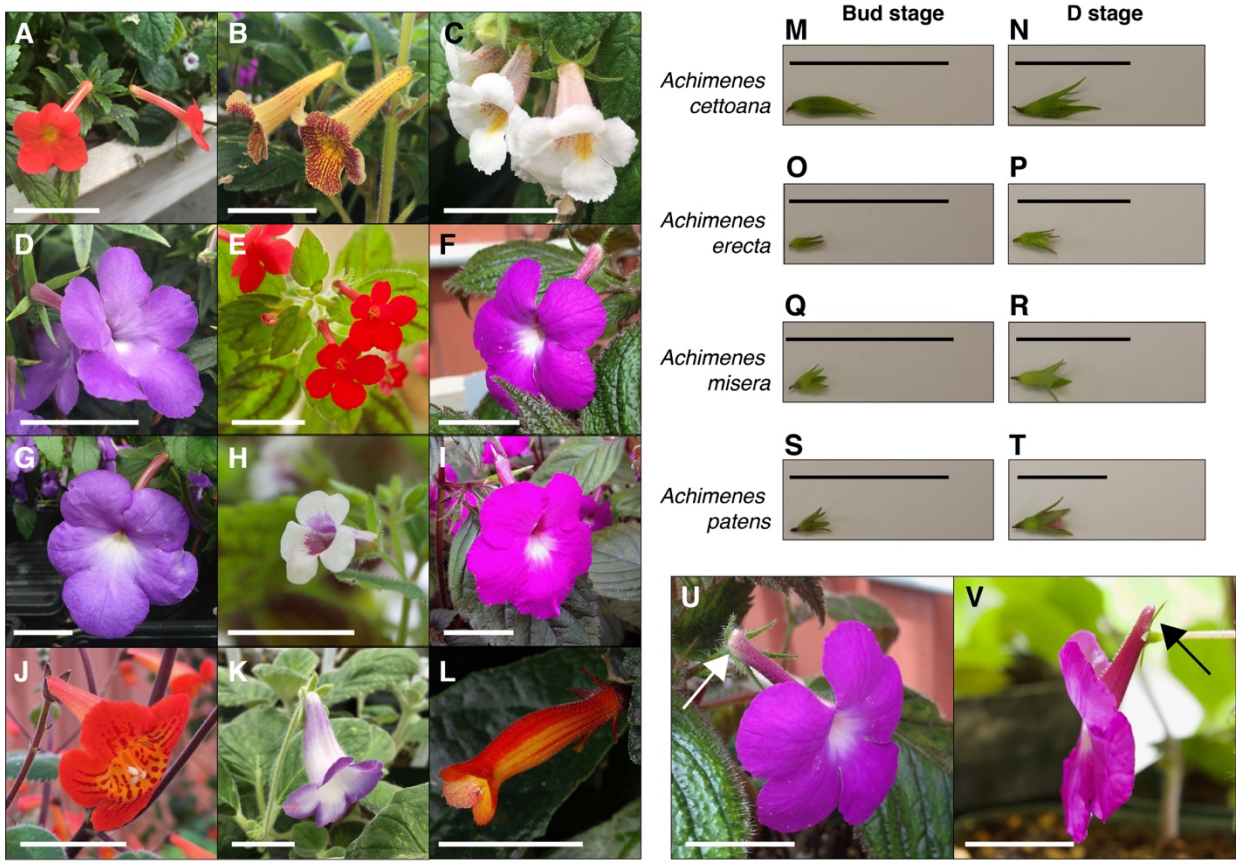

Scale bars equals 1 cm.

Figure 1. *Achimenes* flowers and the sampled developmental stages.

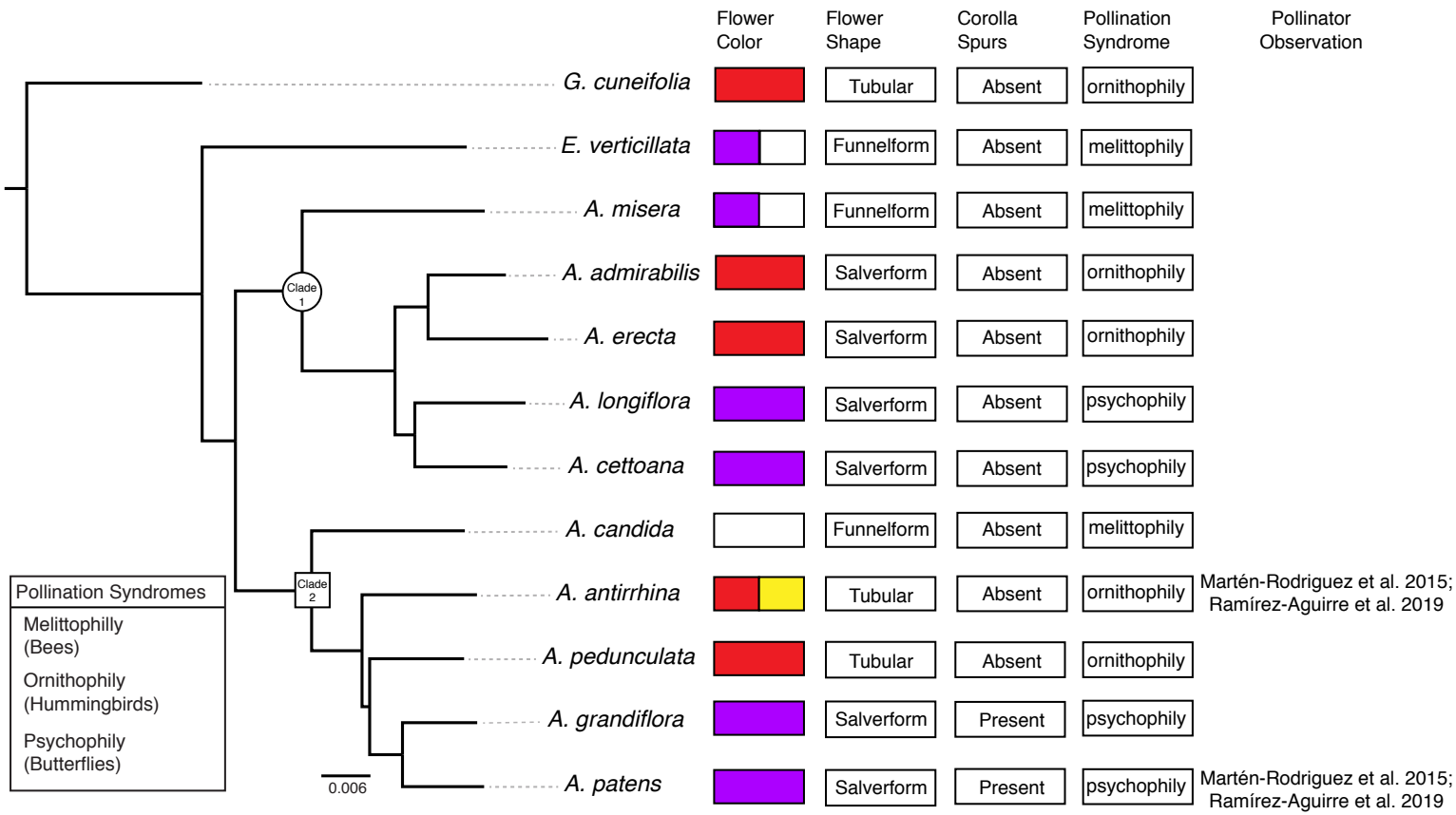

Figure 2. Phylogenetic relationships and floral traits in *Achimenes*.

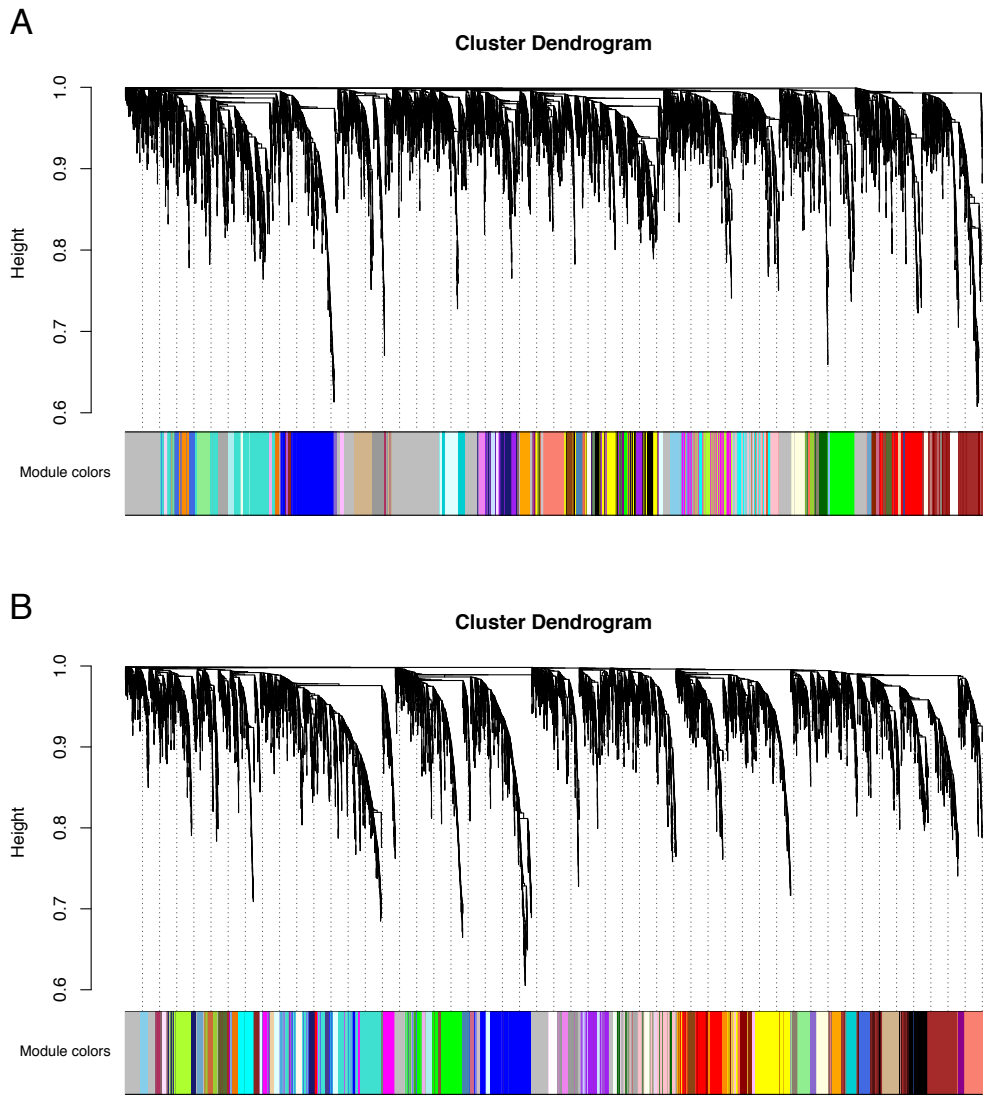

Figure 3. Co-expression clustering of the Bud and D stages.

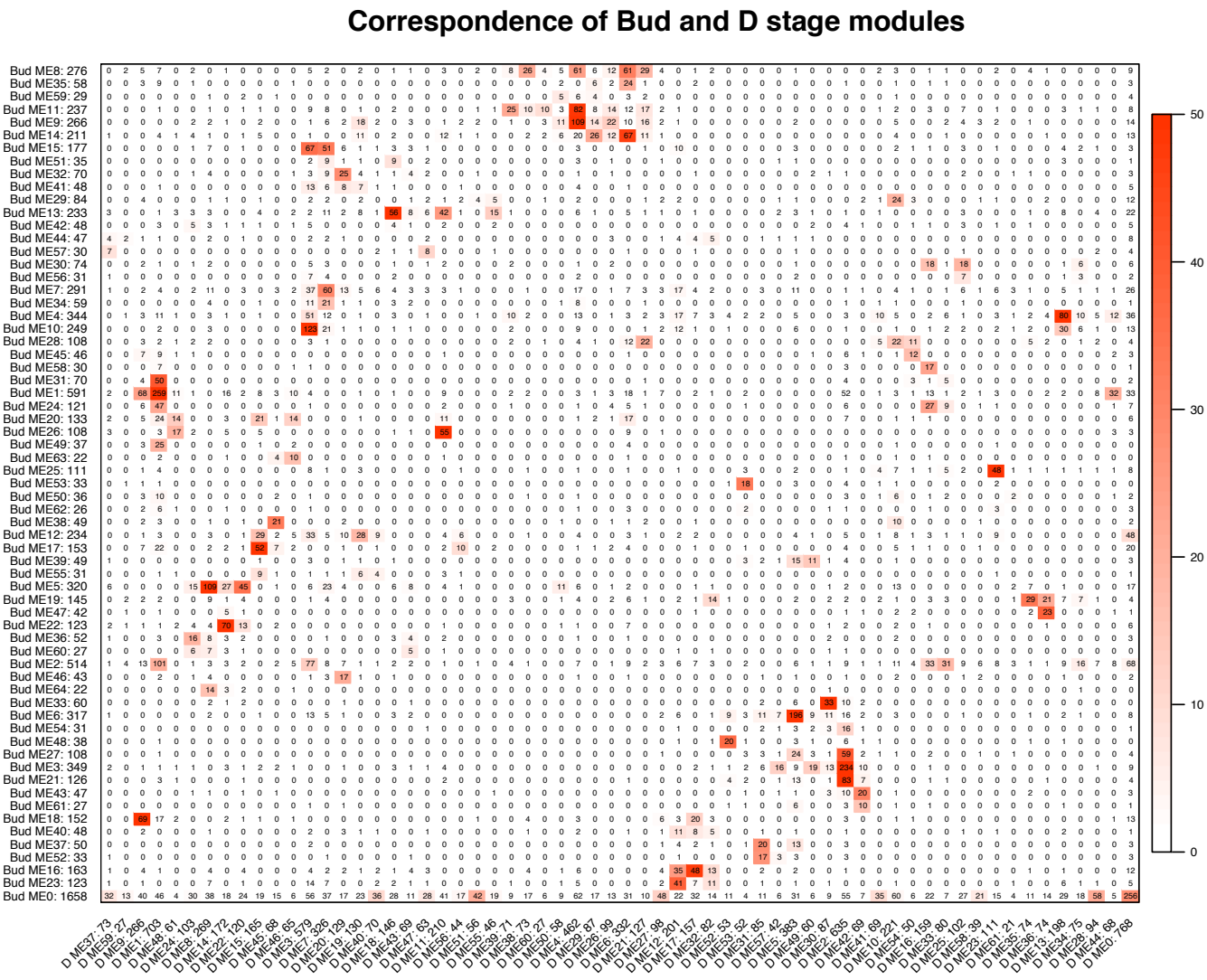

Figure 4. Correspondence of the Bud and D stage networks.

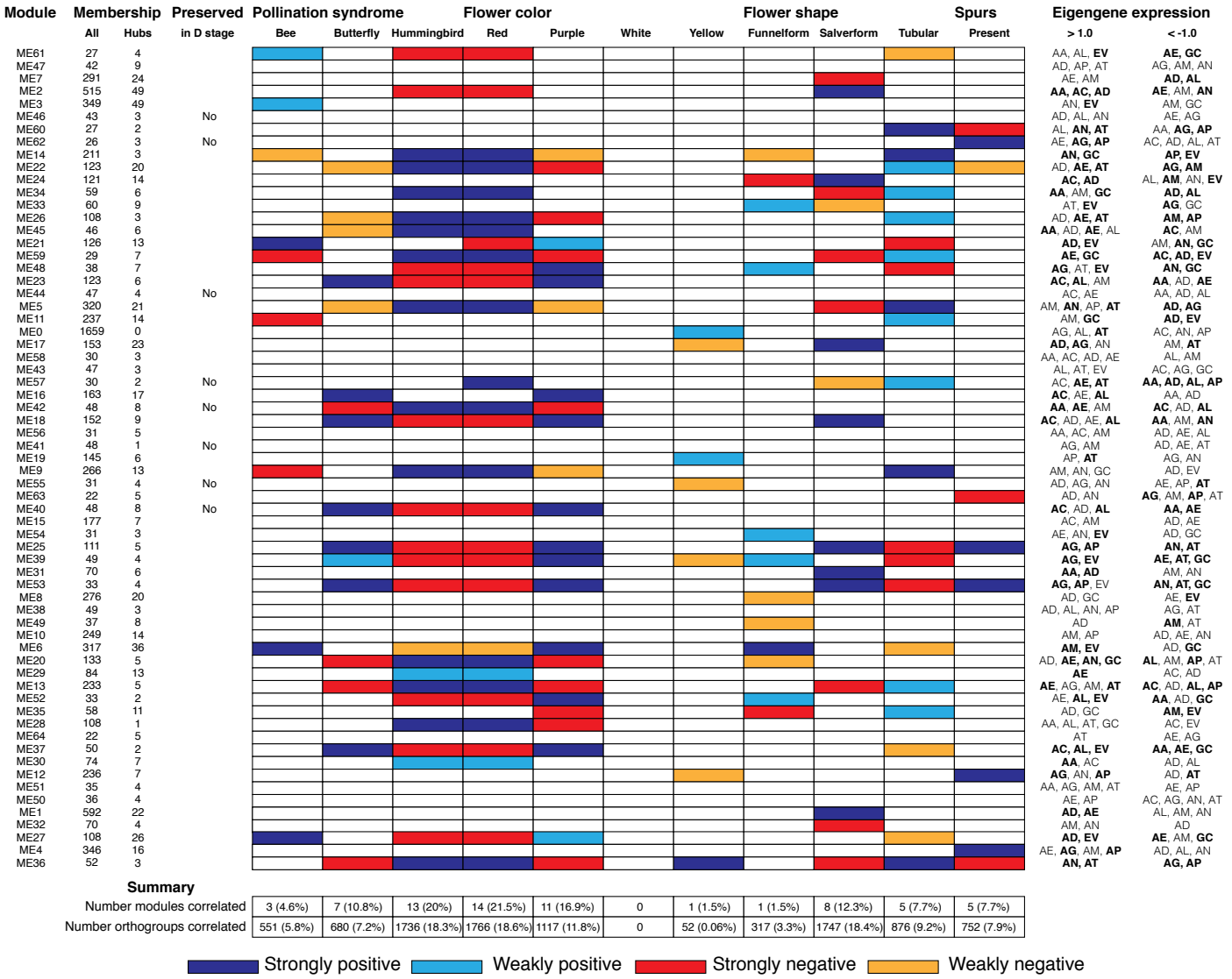

Figure 5. Summary of Bud stage network module association to floral traits and pollination syndrome.

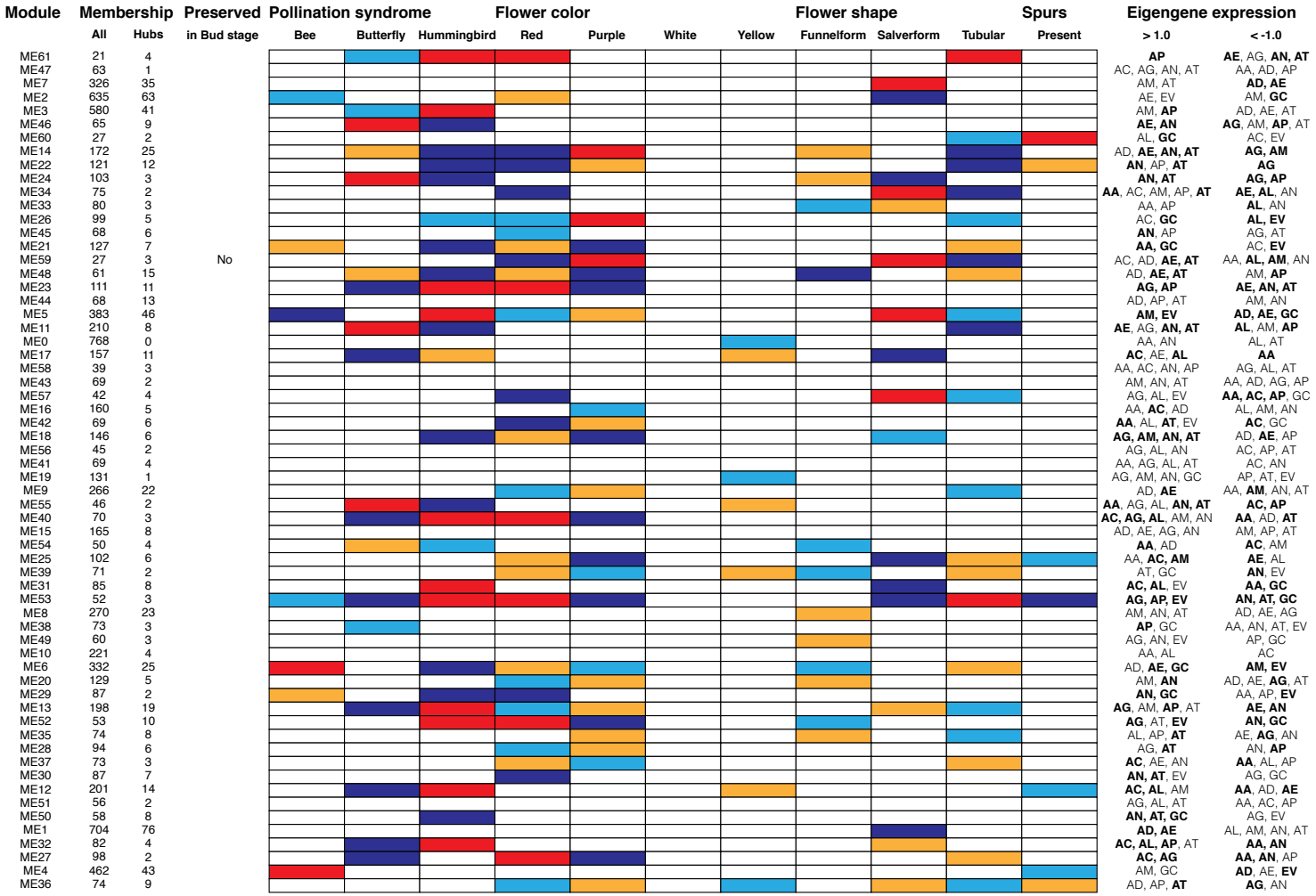

Figure 6. Summary of D stage network module association to floral traits and pollination syndrome.

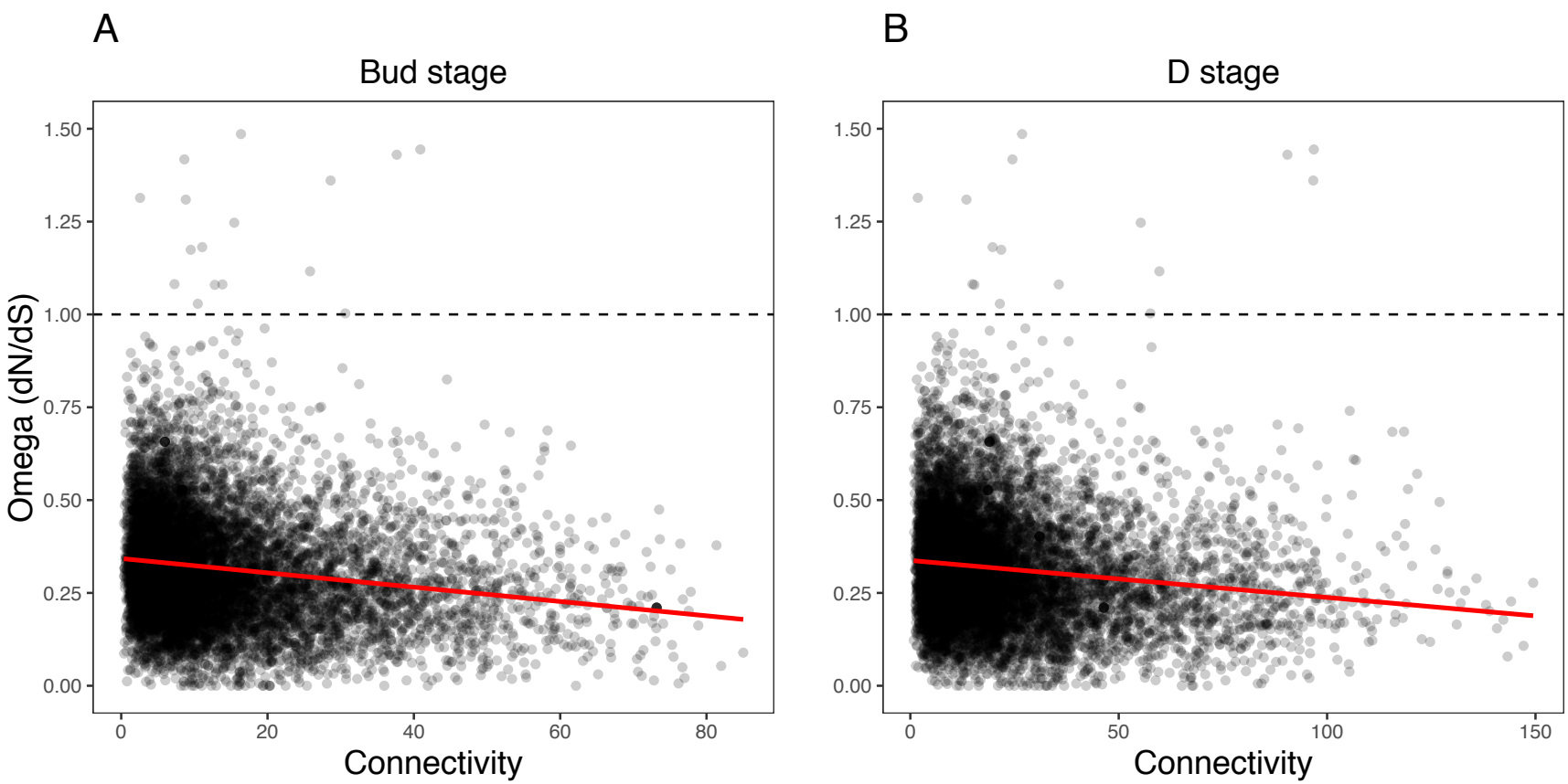

Figure 7. Relationship between orthogroup dN/dS (omega) and orthogroup connectivity.

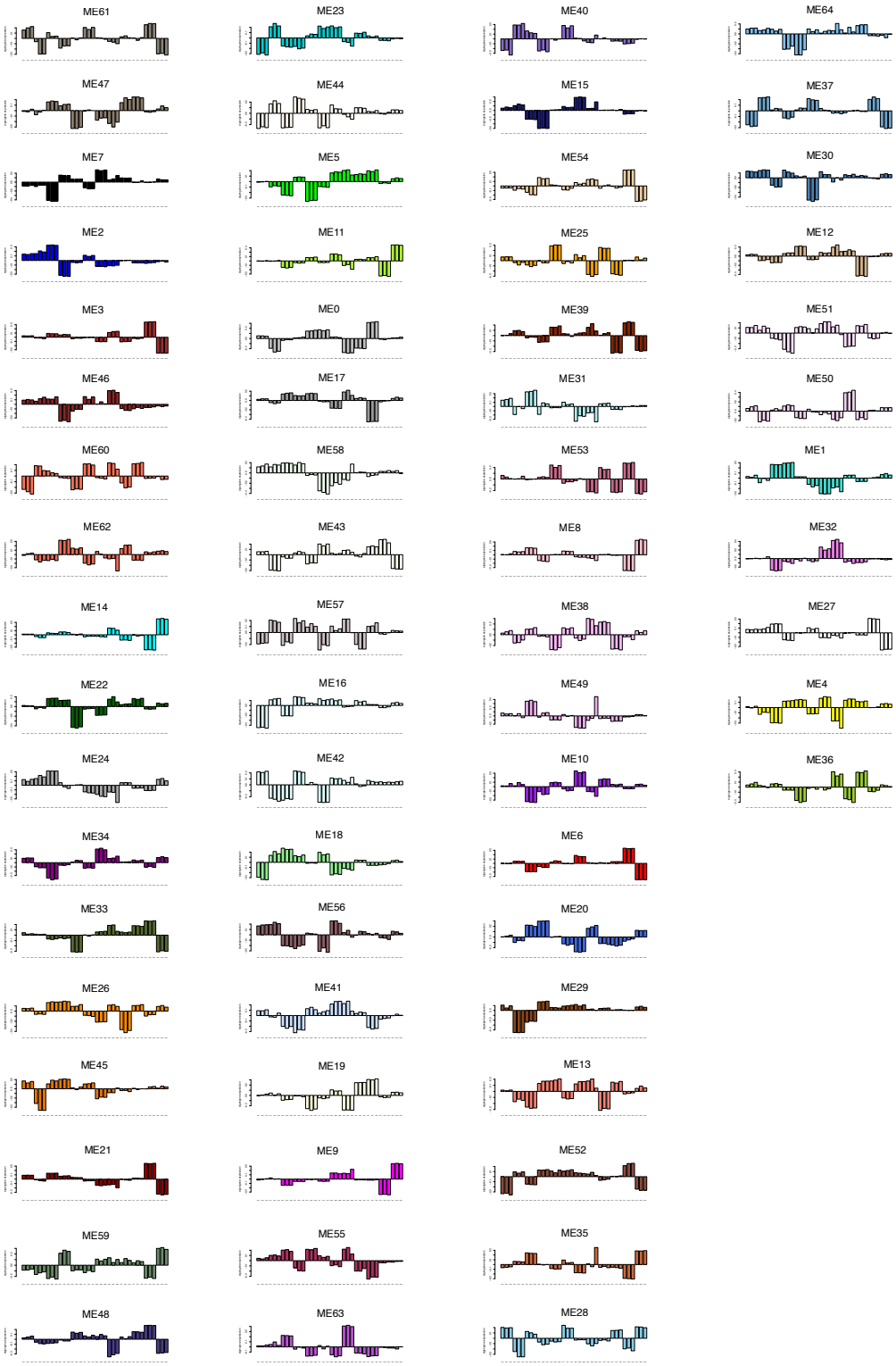

Supplemental Figure 1. Module eigengenes in the Bud stage network.

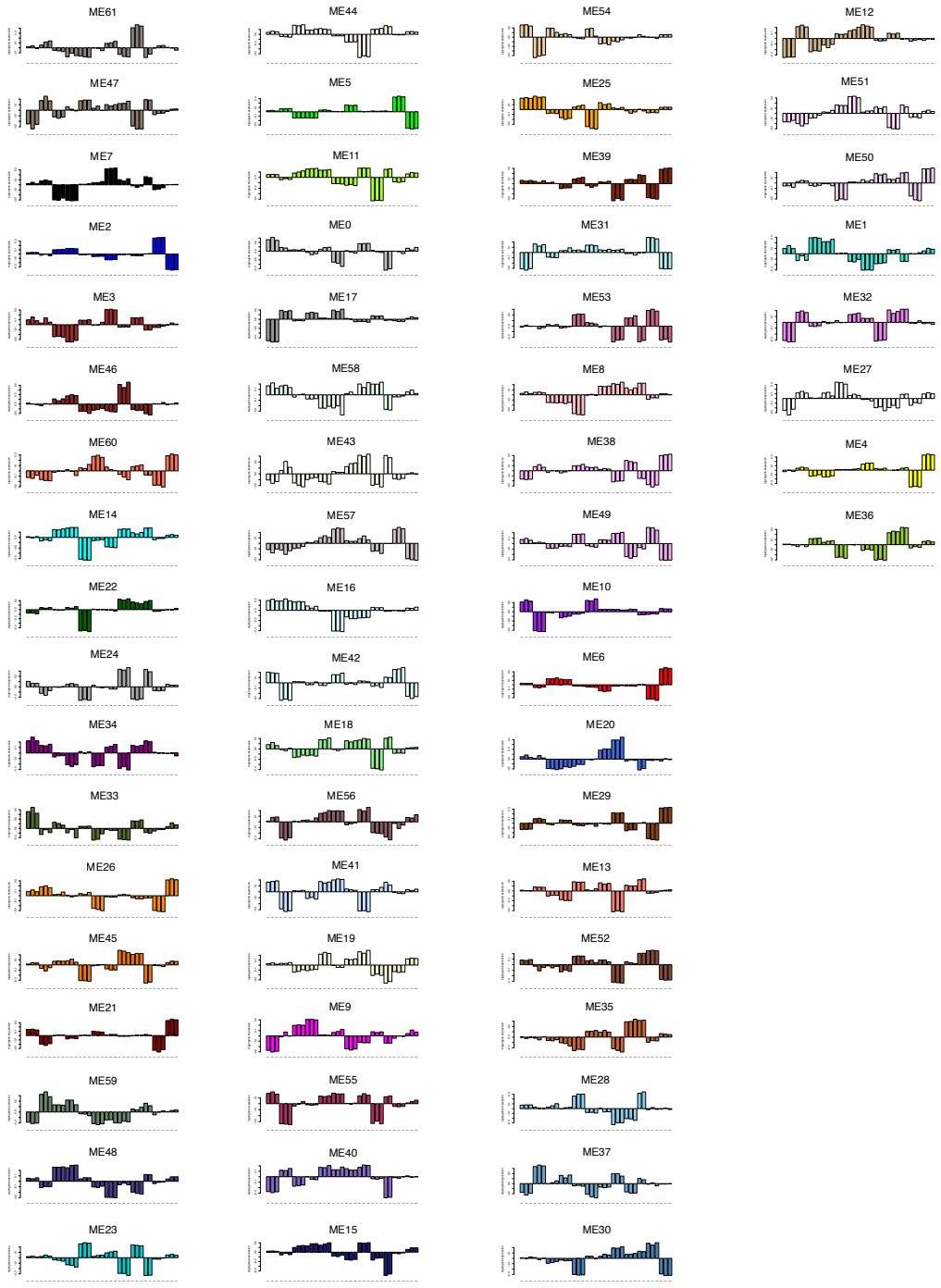

Supplemental Figure 2. Module eigengenes in the D stage network.

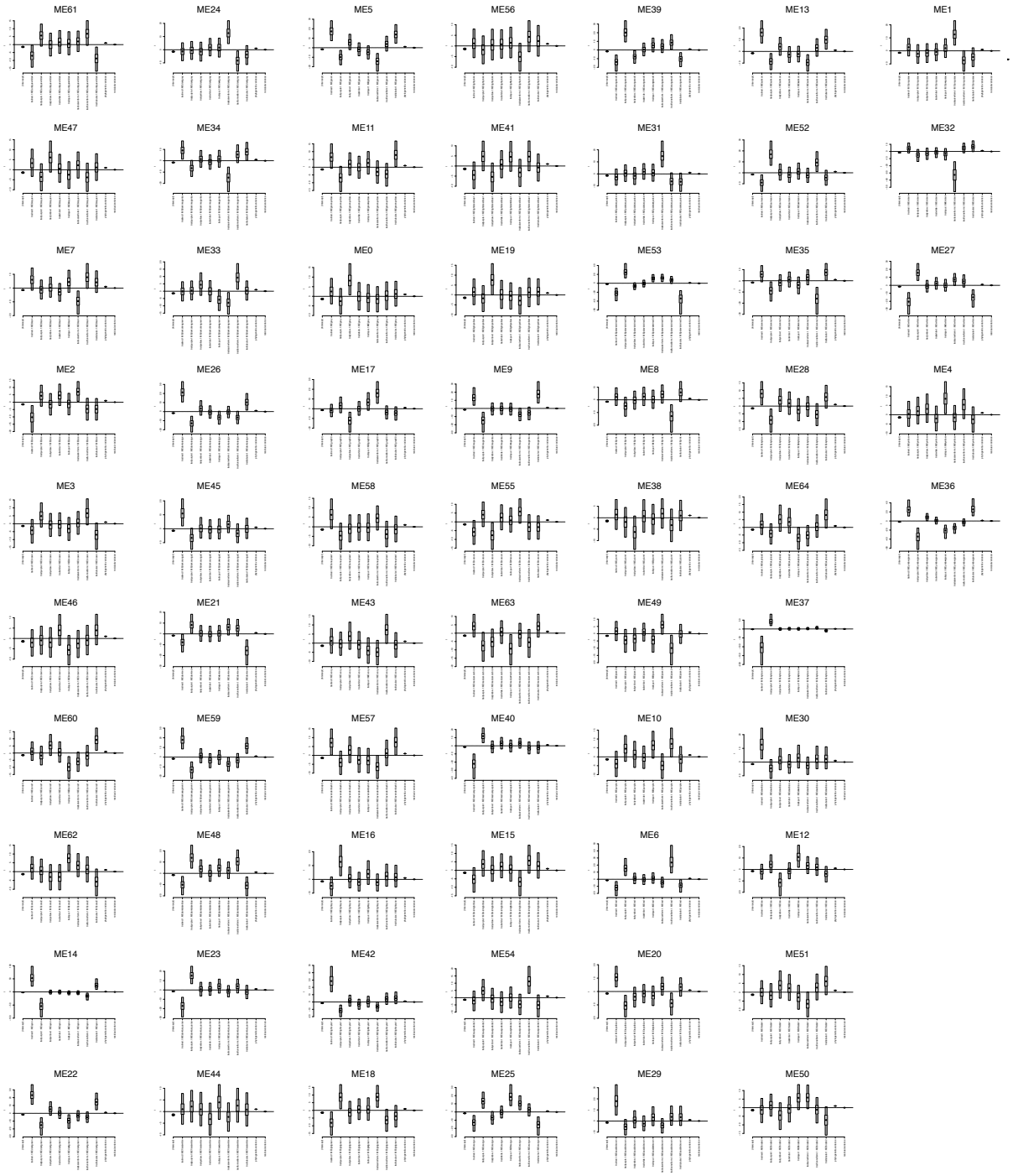

Supplemental Figure 3. Effects of floral traits on the eigengene expression in the Bud stage modules summarized over 50 phylogenetic trees.

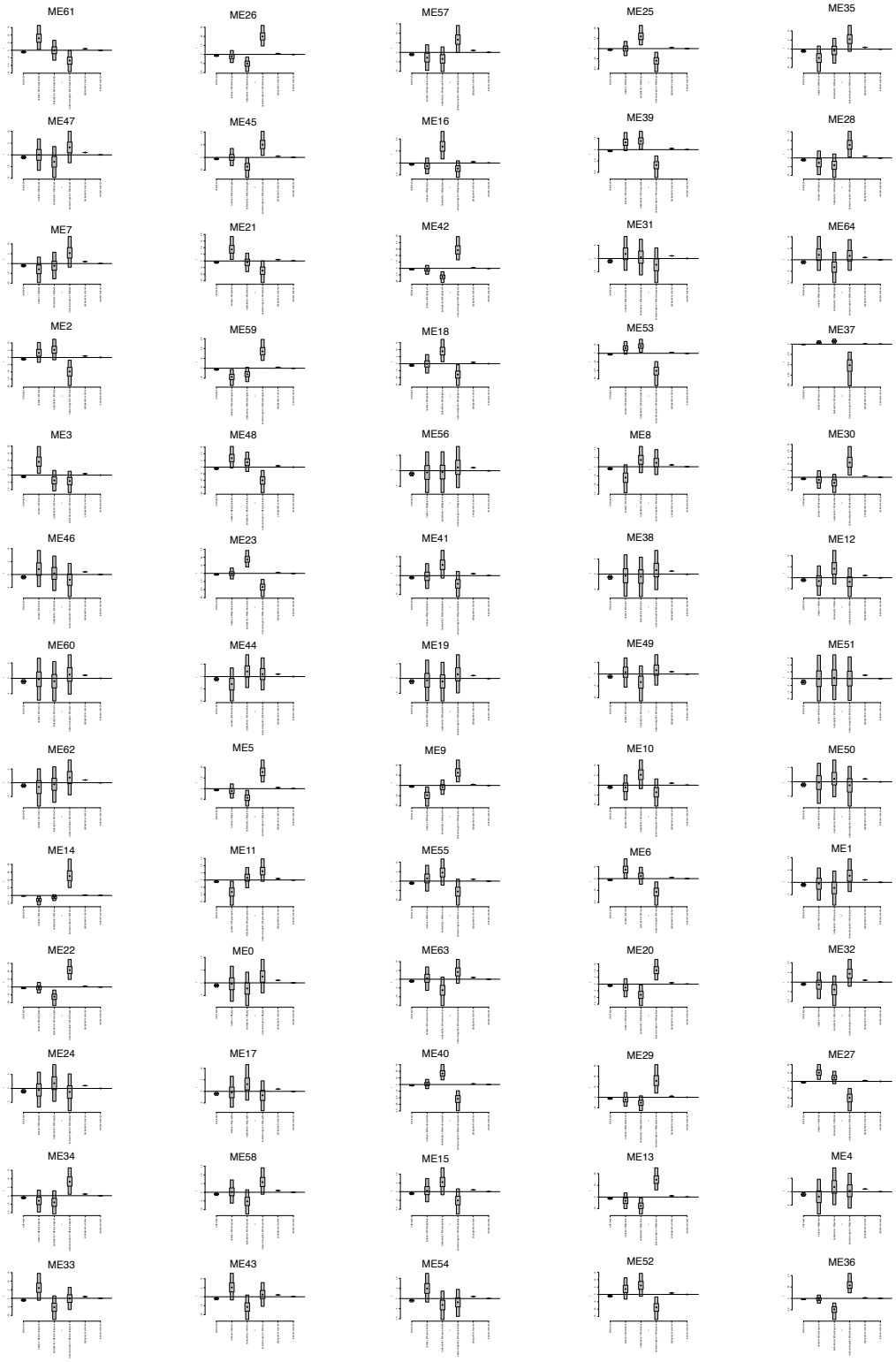

Supplemental Figure 4. Effects of pollination syndrome on the eigengene expression in the Bud stage modules summarized over 50 phylogenetic trees.

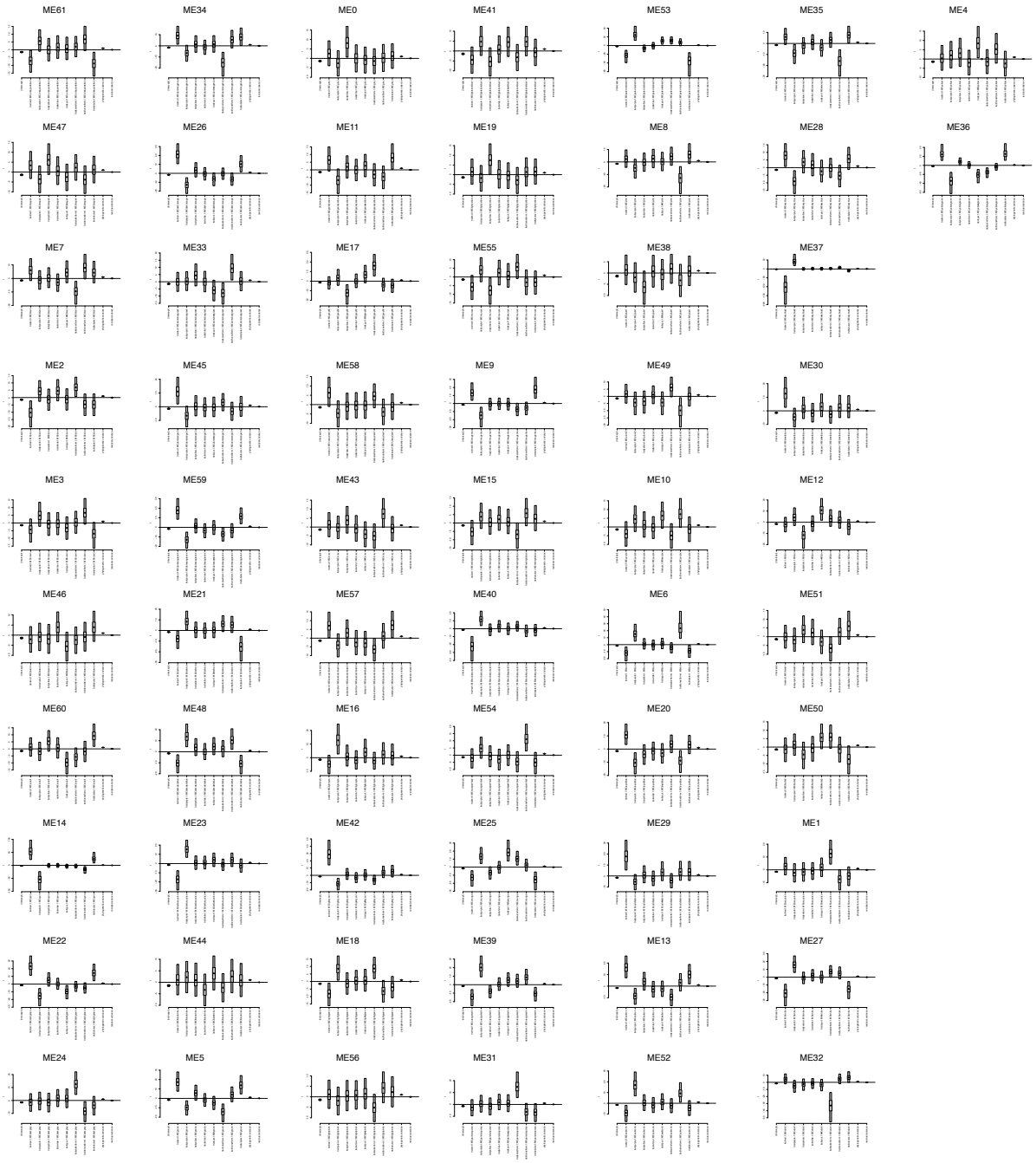

Supplemental Figure 5. Effects of floral traits on the eigengene expression in the D stage modules summarized over 50 phylogenetic trees.

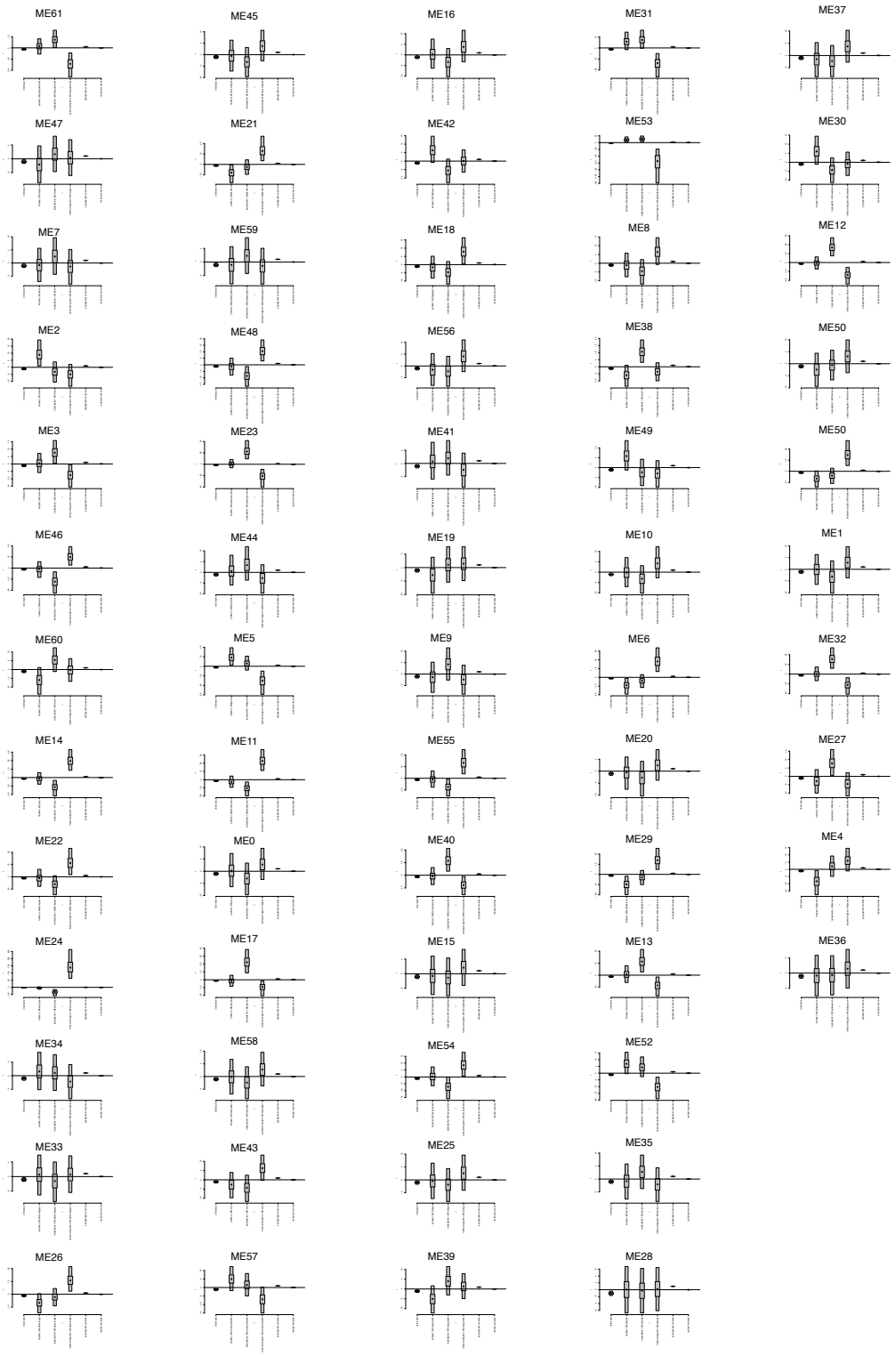

Supplemental Figure 6. Effects of pollination syndrome on the eigengene expression in the D stage modules summarized over 50 phylogenetic trees.

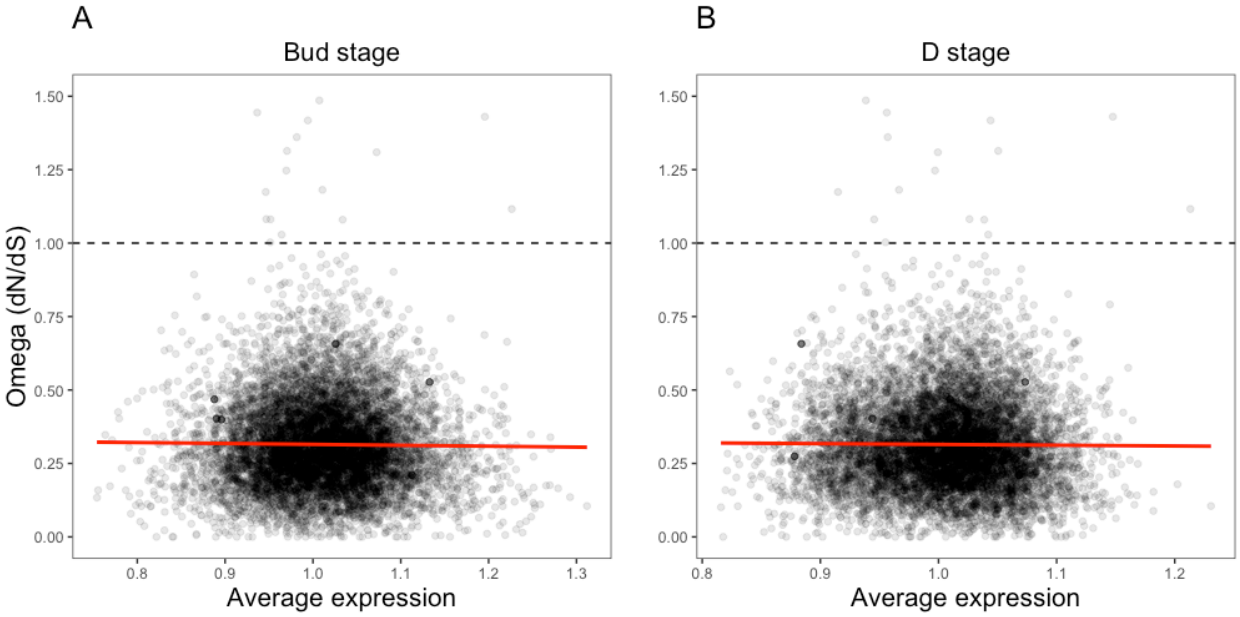

Supplemental Figure 7. Relationship between orthogroup dN/dS (omega) and average expression.

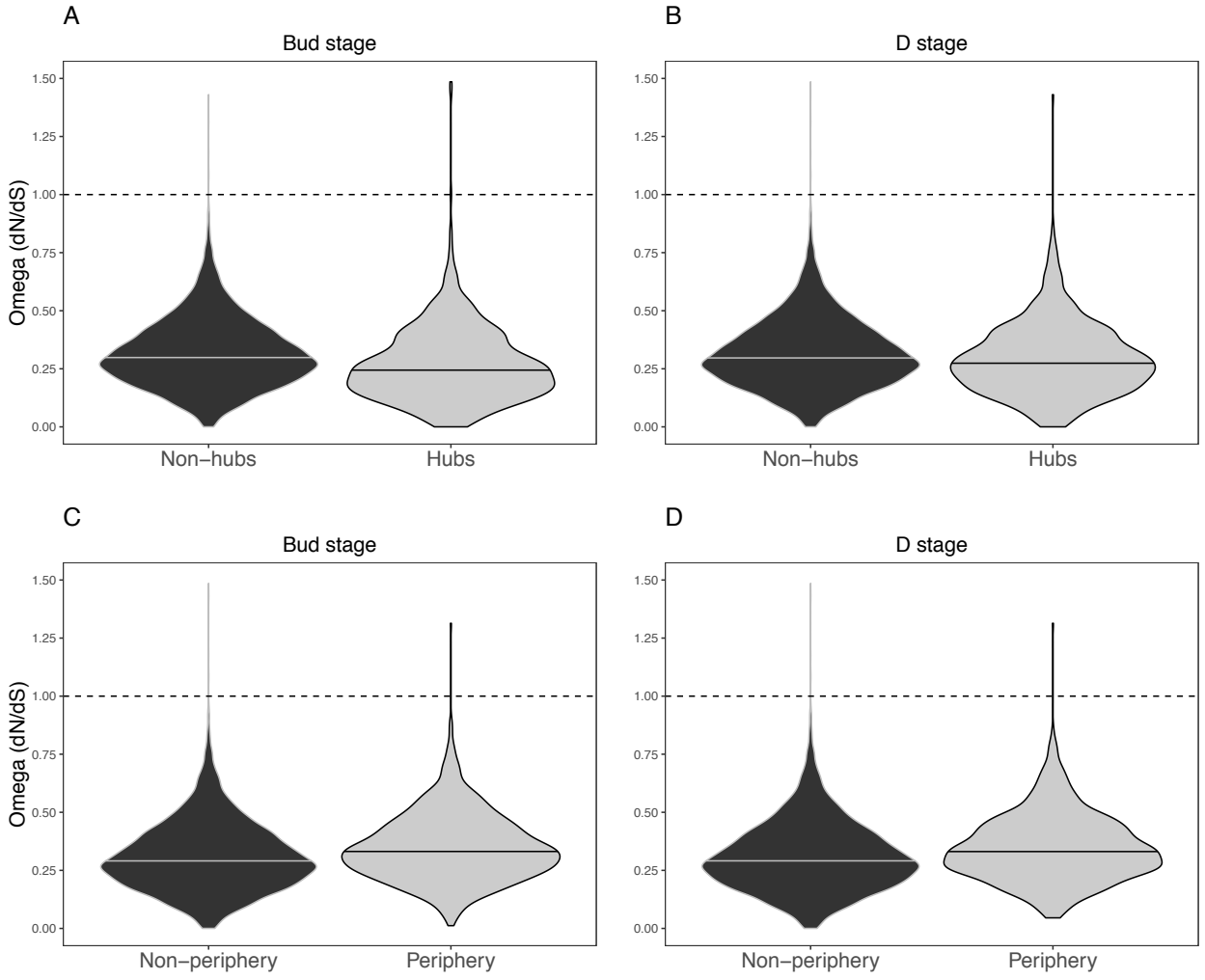

Supplemental Figure 8. Distribution of dN/dS (omega) among hubs and periphery nodes.